Tectonophysics 761 (2019) 65–85

Contents lists available at ScienceDirect

Tectonophysics

journal homepage: www.elsevier.com/locate/tecto

Mesoarchaean-Palaeoproterozoic crustal-scale tectonics of the central Witwatersrand basin - Interpretation from 2D seismic data and 3D geological modelling

Marcello G. Molezzi*, Kim A.A. Hein, Musa S.D. Manzi

School of Geosciences, University of the Witwatersrand Johannesburg, PBag 3, 1 Empire Street, WITS 2050, Gauteng, Johannesburg, South Africa

ARTICLE INFO

Keywords:
Reflection seismics
Witwatersrand Basin
Tectonics
3D geological modelling

ABSTRACT

The Witwatersrand Basin represents one of the largest exposures of Meso-Neoarchaean rock on Earth and hosts the Vredefort Dome at its geographic centre. The southern half of the basin is covered by thin Palaeozoic to early Mesozoic marginal sequences of the Karoo Supergroup. However, visualisation and analysis of this unexposed portion of the basin can be achieved in a 3D geomodelling environment through the integration of geophysical (2D reflection seismics) and traditional geological data. In this study, the 3D structural architecture around the Vredefort Dome in the Witwatersrand Basin is evaluated to establish strato-tectonic relationships, first-order scale structures, and a new model for the architecture of basement rocks. From the geological modelling, several strato-structural features have been identified in the seismic sections, including a well-developed listric fault system in the southwest, a prominent fold system observed in the Transvaal Supergroup, and a large listric fault in the east that offsets the aforementioned fold system. Integration of these geophysical and geological data (in 3D space) has provided 3D constraints on the volumes for the Witwatersrand Supergroup, Ventersdorp Supergroup and Transvaal Supergroup to the south, southeast and east of the Vredefort Dome.

1. Introduction

Geomodelling as a visualisation and analysis tool is a powerful method for many types of geological work. As stated by Jones et al. (2009), the preservation of data at all scales within one computer-based 3D spatial interface is the primary advantage of multi-scaled 3D geological modelling. Through this aspect, geological data of all types and scales must be brought together to form the geological architecture of a given terrane. Geophysical data (e.g. magnetics, gravity, and seismics) can be used in conjunction with both geochemical (e.g. soil sampling, rock chip sampling, and geochronology) and traditional geological data (e.g. mapping, drilling, cross sections, stratigraphy, and petrography) to provide new models. In a 3D geomodelling environment these datasets can be integrated in various ways potentially giving new insights into the geology of the Earth's crust, particularly in regions under sedimentary cover.

In this paper the term “Witwatersrand Basin” reflects the multi-basin rock record located towards the centre of the Kaapvaal craton. The “basin” represents several different, successor basins deposited over span of time (Mesoarchaean to Palaeoproterozoic eras) extending beyond the deposition of the basins recorded in the Witwatersrand Supergroup. Specifically, these basin fills are recorded in the Dominion Group, Witwatersrand Supergroup, Ventersdorp Supergroup, and Transvaal Supergroup.

The Witwatersrand Basin contains one of the best documented gold provinces in the world. Its tectonic history is understood broadly although it lacks geometry and kinematic data that would help establish the geodynamic development of the basin (Dankert and Hein, 2010). The basin hosts one of the largest exposures of Meso-Neoarchaean rock on Earth and includes the Vredefort Dome at its geographic centre representing the largest (250–300 km wide) and possibly oldest (2023 ± 4 Ma; Kamo et al., 1996) confirmed impact crater on Earth. However, relative to the known extents of the basin, the Meso-Neoarchaean sequences are only exposed at surface in the north (Fig. 1). Towards the south the Witwatersrand Basin is covered by thin Palaeozoic to early Mesozoic marginal sequences of the Karoo Supergroup. Geological interpretations of the Witwatersrand Basin beneath this cover have been limited to borehole and 2D geophysical data, with rare exposures as inliers where the Karoo cover has been eroded, making a fuller understanding of the basin difficult.

Several integrated geological and geophysical 2D models have been constructed to create models of the first-order structural architecture of

* Corresponding author.
E-mail addresses: marcello@mgmgeoservices.com (M.G. Molezzi), kim.hein@wits.ac.za (K.A.A. Hein), musa.manzi@wits.ac.za (M.S.D. Manzi).

https://doi.org/10.1016/j.tecto.2019.04.004
Received 29 November 2018; Received in revised form 23 March 2019; Accepted 7 April 2019

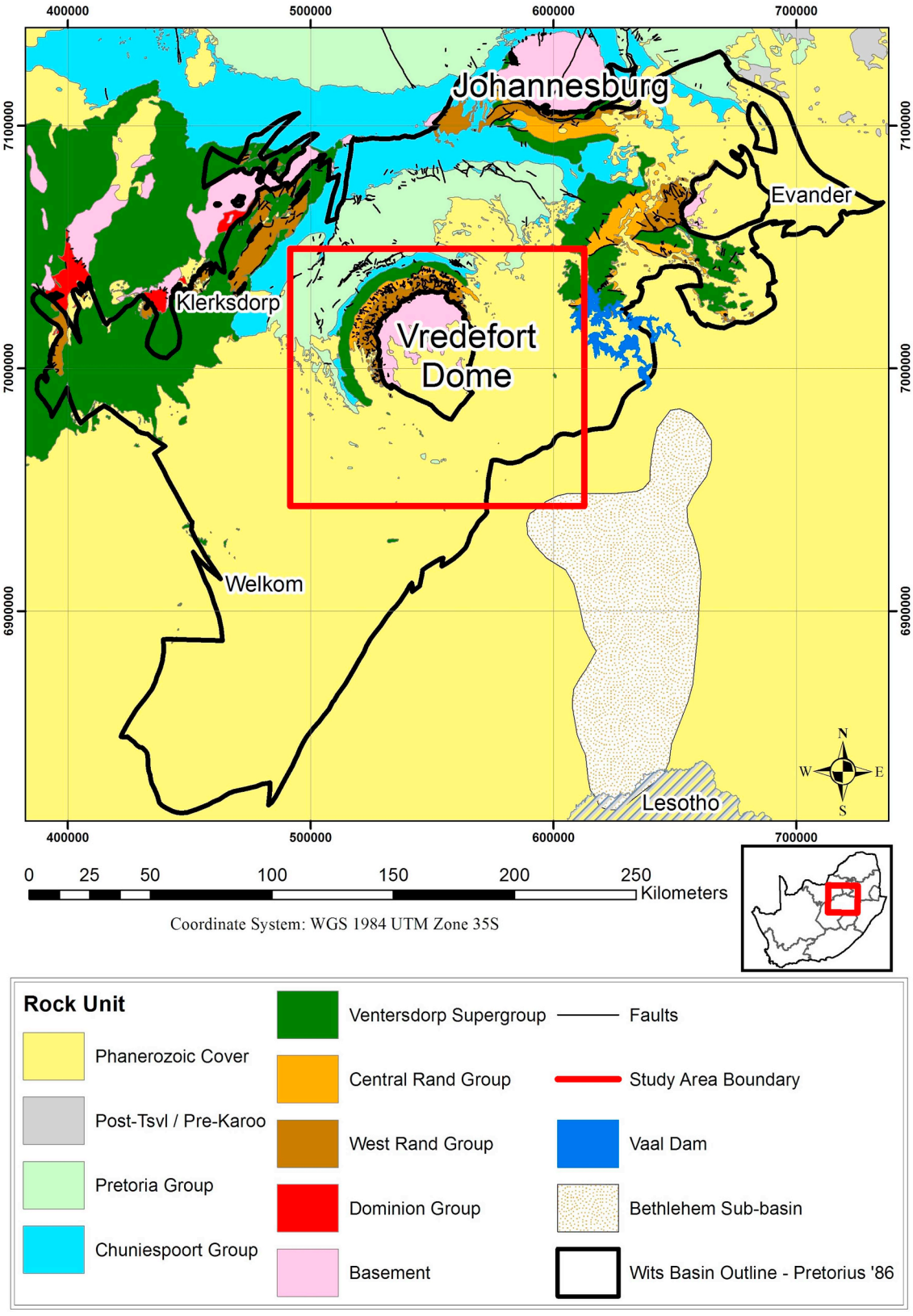

Fig. 1. Regional geology map with the study area boundary, including the interpreted extent of the Witwatersrand basin after Pretorius (1986), and the outline of the Bethlehem sub-basin gravity anomaly.

the Vredefort Dome and the Witwatersrand Basin. Henkel and Reimold (1998) used magnetic and gravity profiles to model the dome and part of the Witwatersrand Basin, with added constraints from associated two reflection seismic profiles. From their two seismic sections they interpreted tilting of the post-impact crust to the northwest, and northwest-directed thrust shortening and uplift of the southeast portion of the dome. This concurs with previous interpretations by Friese et al. (1995) who used 2D reflection seismic and gravity data to create

models through the dome and across the Witwatersrand Basin.

Beach and Smith (2007) and Manzi et al. (2013) created first-order scale models of the structural architecture using high-resolution 3D reflection seismic data and emphasised the role of fold-thrust tectonics during development of the Witwatersrand Basin, and later, extension tectonics and the formation of listric faults during formation of the Ventersdorp Supergroup. However, integration of geological data in 3D using the numerous 2D reflection seismic profiles in the vicinity of the dome and southeast Witwatersrand Basin has not been attempted before and could provide greater accuracy in representations of the structural architecture of the dome, and its formation.

In this study we take advantage of extensive borehole databases, and geophysical surveys (focussing on legacy 2D reflection seismics, with qualitative input from magnetics and gravity) to constrain the geometry of the Vredefort Dome at depth. Thus, a 3D geological model of the Vredefort Dome and immediate surroundings is presented. The advantage of an integrated 3D model of the dome is that it can be queried and easily updated as new data becomes available.

The 3D structural architecture around the Vredefort Dome in the Witwatersrand Basin is evaluated, particularly the unexposed portion, to establish strato-tectonic relationships, first-order scale structures, and the general basement architecture. The objectives establish a comprehensive database for the dome, including datasets for drilling, geological and structural mapping, geophysics, and topographic elevation models. The quality of the legacy 2D reflection seismic data is also evaluated and provides interpretations of the 2D seismic sections, with a focus on the major unconformities.

We query the existing strato-tectonic history of the Witwatersrand Basin through integration of surface mapping, drilling, seismic data interpretations and geological modelling. The architecture of the contact Kaapvaal basement and the Witwatersrand Basin has therefore been updated to include depth variations around the dome and first-order cross-cutting structures. It has also been possible to establish the extent of the unexposed Witwatersrand Supergroup, Ventersdorp Supergroup and Transvaal Supergroup to the south, southeast and east of the dome.

2. Regional geology

The Witwatersrand Basin is situated in South Africa and unconformably overlies Palaeo-Mesoarchaean basement rocks to form part of the Kaapvaal craton. Several stratigraphic units are described below that correspond with the regional geology map in Fig. 1. The units form the modelled volumes following interpretation of the 2D reflection seismic data. Fig. 2 illustrates these units in relation to the expected seismic reflective boundaries in the seismic sections. The cratonic basement is made up of discrete terranes dated at ca. 3.6–3.2 Ga (U-Pb ID-TIMS and SHRIMP, and Pb-Pb zircon evaporation, Poujol et al., 2003). The basement is composed of tonalite–-trondhjemite–granodiorite (TTG) suites and greenstone belts that outcrop rarely across the craton (Poujol et al., 2003; Johnson et al., 2006).

The stratigraphy (and geochronology) applied to the study area has been summarised by several authors, including Johnson et al. (2006), Dankert and Hein (2010) and Molezzi (2017). The Witwatersrand Basin is situated near the geographic centre of the Kaapvaal craton. Outcrop of the Mesoarchaean portions of the basin are limited to its northern extent (i.e. adjacent to Johannesburg, Klerksdorp, and Evander) and in the collar rocks of the Vredefort Dome. The package overlying the basement (and Dominion Group) is made up of several successor basins and stratigraphic units that span ca. 2.98–2.02 Ga and form part of three major supergroups, namely, the Witwatersrand Supergroup, Ventersdorp Supergroup, and Transvaal Supergroup. The base formations of these basins form major unconformities with the underlying basins, e.g., the Venterspost Contact Formation (VCF), the base of the Central Rand Group, and the Black Reef Formation. The ca. 300–180 Ma Karoo Supergroup also exhibits a major unconformably as progressive termination of the major supergroups against it is mapped across the study area.

Several tectonic regimes have affected the Kaapvaal craton throughout the Mesoarchaean, Neoarchaean and Palaeoproterozoic. Following basement complex stabilisation, the deposition of the Dominion Group took place synchronous to continental rifting in an overall arc setting (Frimmel et al., 2009). Nearly 100 million years later, passive margin basin formation was initiated with synchronous deposition of the West Rand Group (Johnson et al., 2006; Dankert and Hein, 2010). The Asazi Event terminated sedimentation, and the craton underwent uplift and tilting syn- to post-peneplanation, including local faulting and block tilting (Dankert and Hein, 2010; Manzi et al., 2013). Extensional tectonics gave way to fold-thrust belt formation, which Frimmel (2014) interpreted as forming a retroarc, and the Central Rand Group was deposited. Dankert and Hein (2010) stated that the Umzawami Event took place synchronous to, and/or after the deposition of the Central Rand Group. This event was defined by basin-wide development of folding, identified in the Central Rand Group sedimentary rocks.

Following cessation of retroarc development, the Kaapvaal craton underwent peneplanation and degradation of the basin margin to form the auriferous conglomerate horizons of the Venterspost Formation. The sedimentation took place 120 million years after deposition of the Mondeor Formation (youngest formation of the Central Rand Group). This transition phase culminated in a major continental rift regime, where crustal extension produced the nearly craton-wide volcanism of the Klipriviersberg Group. The continued extensional collapse is described by Manzi et al. (2013) as the Hlukana-Platberg Event, and included major graben formations, reactivation of pre-existing structures as listric faults, and associated sedimentation of the Platberg Group. A period of erosion and excision followed the final deposition of the Bothaville Formation and Allanridge Formation (Frimmel, 2014).

Several other structural indicators are grouped by Dankert and Hein (2010) as the Ukubambana fold-thrust belt event. These indicators include folds, faults and auriferous quartz veins crosscutting the Timeball Hill Formation, and discrete hydrothermal activity. The event was tentatively constrained to a 200 million year time period subsequent to, and/or during deposition of the upper Pretoria Group (ca. 2.2–2.0 Ga). However, the same structural and petrofabric indicators were formerly ascribed to the Transvaalide orogeny, thrust-fold belt by Alexandre et al. (2006). They were able to resolve two distinct events within the Transvaalide belt, having obtained two sets of $^{40}Ar/^{39}Ar$ ages, one of ca. 2150 and another of 2042.1 ± 2.9 Ma. These ages were for syn-kinematic mica taken from phyllitic rocks of the Timeball Hill Formation west of Pretoria.

The 1.7 billion year hiatus between the Pretoria Group and overlying Karoo Supergroup highlights a major unconformity. The rock record from this extended time period is absent apart from dykes and sills of the Pilanesberg Complex dyke swarm at 1310 ± 60 Ma (Van Niekerk, 1962) and the Anna's Rust Sheet monzodiorite at ca. 1.05 Ga (Johnson et al., 2006; Reimold and Koeberl, 2014). The Karoo-aged dykes are widespread across the basin and are feeders of the continental flood basalts that covered much of southern Africa at ca. 180 Ma. This extensional regime corresponds with the major rifting event associated with the breakup of the Pangea Supercontinent, ca. 180 Ma (Catuneanu et al., 2005).

3. Methods

The methodical framework used in this study is given in Fig. 3 and is organised into four phases. The general framework was an adaptation of the framework presented by Kaufmann and Martin (2009). Borehole,

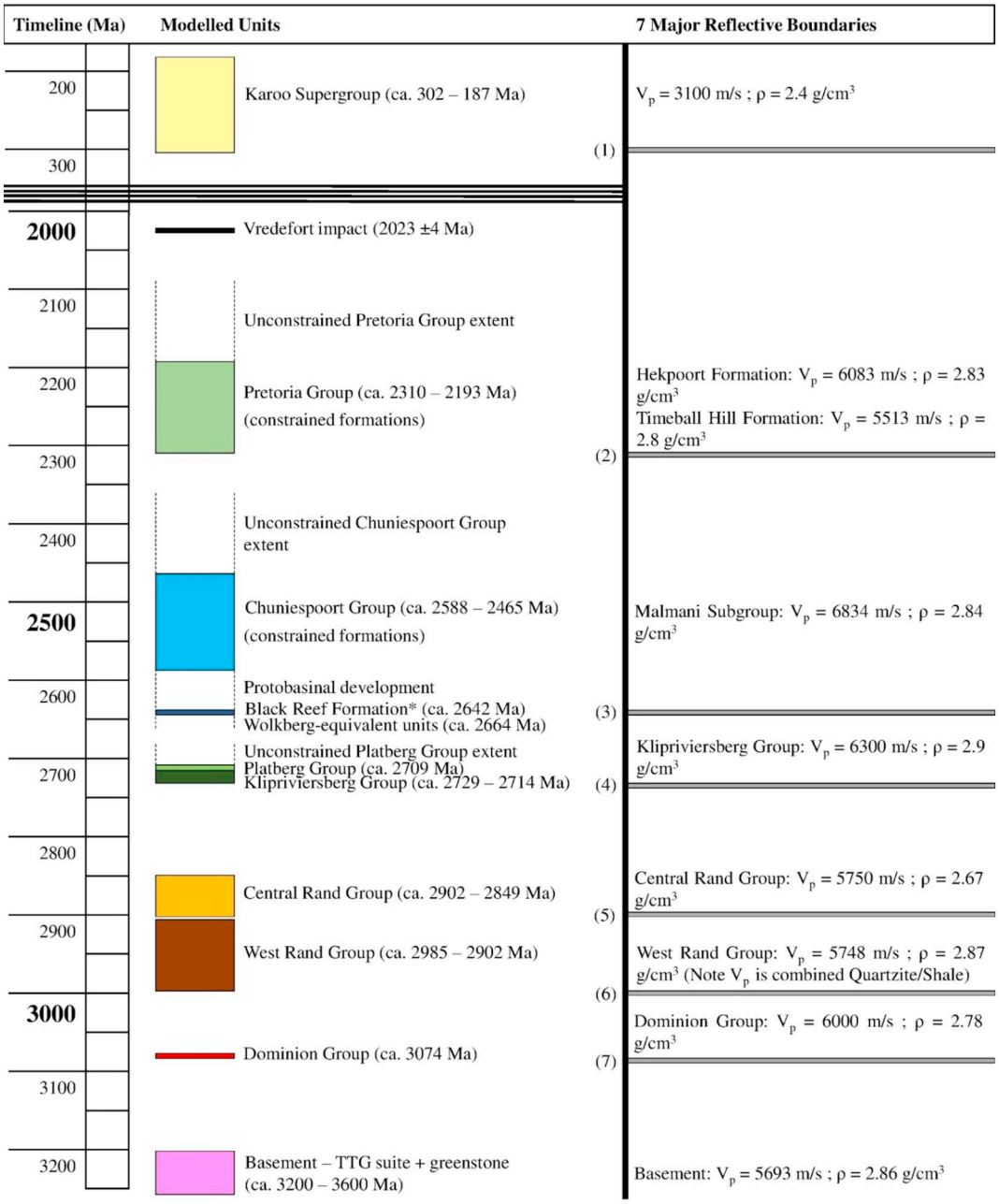

Fig. 2. Summary of main stratigraphic units (as illustrated by Johnson et al., 2006) interpreted in the 2D reflection seismic sections, including the major reflector boundaries imaged in the sections (with associated Vp and ρ estimates from values in Table 1, based on the rock proportions for each measured stratigraphic unit). The Hekpoort and Timeball Hill formations form a minor reflective boundary between them but are not pronounced enough to confidently form separate units. The Platberg and Klipriviersberg groups were combined as a single unit in the interpretations. Note, the extent of each unit is set by geochronological constraints of the dated formations. However not all formations are constrained, therefore stippled lines indicate unconstrained formations exist.

surface mapping and 2D reflection seismic data were imported into Leapfrog Geo® and used for geological interpretations. Most importantly, the borehole data were used to constrain the interpretation of strong reflections observed on the seismic sections. These interpretations were digitised, and a 3D geological model was constructed together with support wireframes. For a more detailed description of the various methods used the reader is referred to the online Supplementary material. A few extra citations in this material are not in the manuscript, these include Armstrong et al. (1991), Chopra et al. (2006), Henneing and Paton (2012), and Kositcin and Krapeˇz (2004).

3.1. Phase 1

3.1.1. Surface information: topographic data, geological maps, and geophysical images

A 90 m resolution SRTM digital elevation model (Farr et al., 2007) was imported into LeapFrog Geo® to form the 3D topography surface of the study area. Furthermore, the modelling incorporated geological maps, i.e., 1:250,000 and 1:250,000 covering the Vredefort Dome (Coetzee, 1986; Wilkinson, 1986; Smith, 1992; Bisschoff et al., 1999; Retief, 2000), from which a total of 1002 foliation measurements were

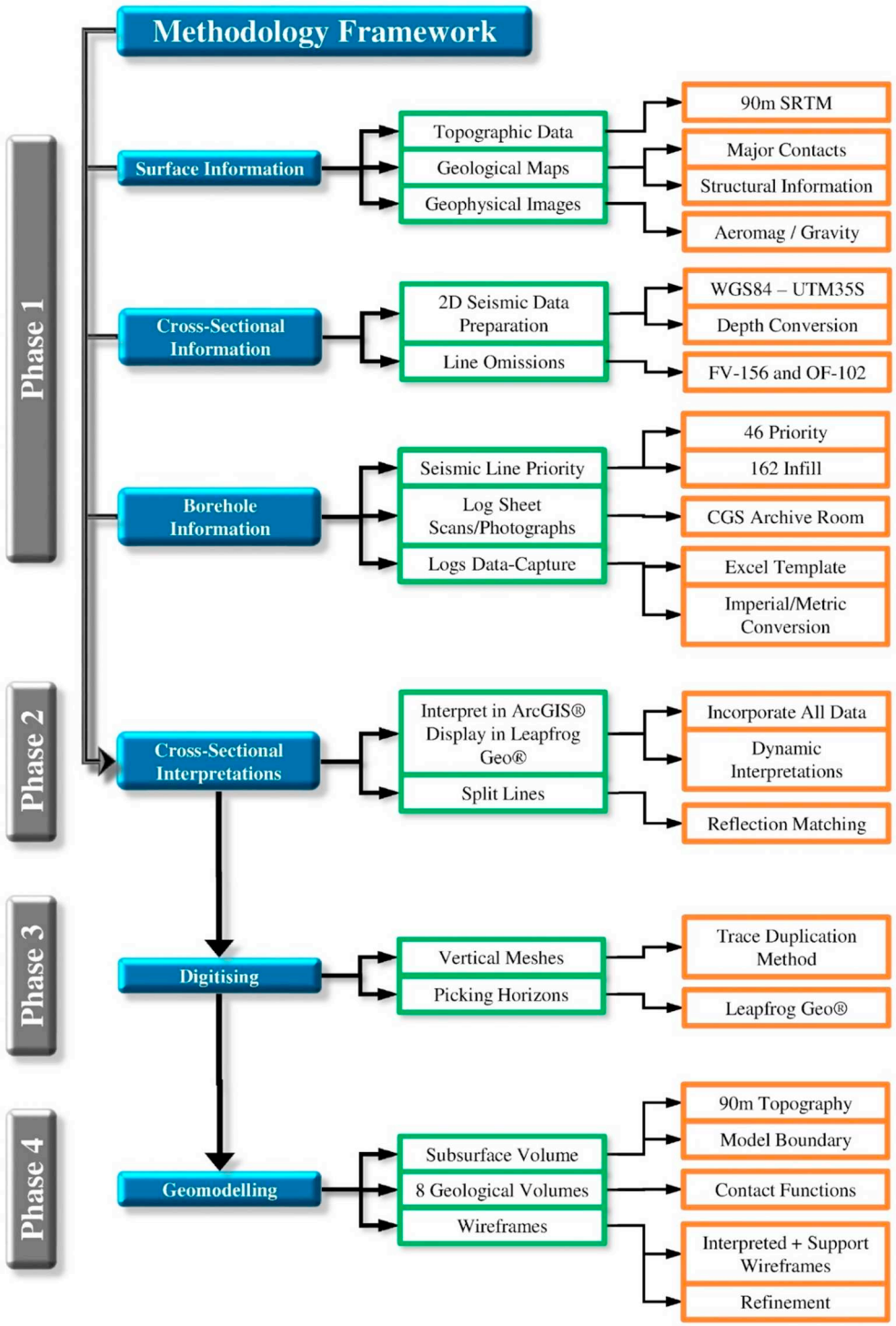

Fig. 3. Methodology framework for the geological modelling.

digitised in ArcGIS®. The structural data were extracted from these maps (1:250,000 scale maps). The magnetic and gravity data were only incorporated qualitatively, as guides during the interpretation and modelling phases. However, future research on this topic should incorporate both magnetic and gravity modelling results in those analyses.

3.1.2. Cross-sectional information: 2D reflection seismic data

The most important parameter that affects the strength of a reflected signal from a geological boundary is the contrast in acoustic impedance, a product of seismic velocity, P-wave (V_p) or S-wave (V_s), and bulk density (ρ). For a lithological boundary to generate a noticeable reflection, the amplitude of a reflected wave (i.e. reflection coefficient, RC) relative to an incident wave should be at least 6% of the incident energy (Salisbury et al., 2003). The RC is represented by the following equation:

$$RC = (\rho 2V2 - \rho 1V1)/(\rho 2V2 + \rho 1V1)$$

where,

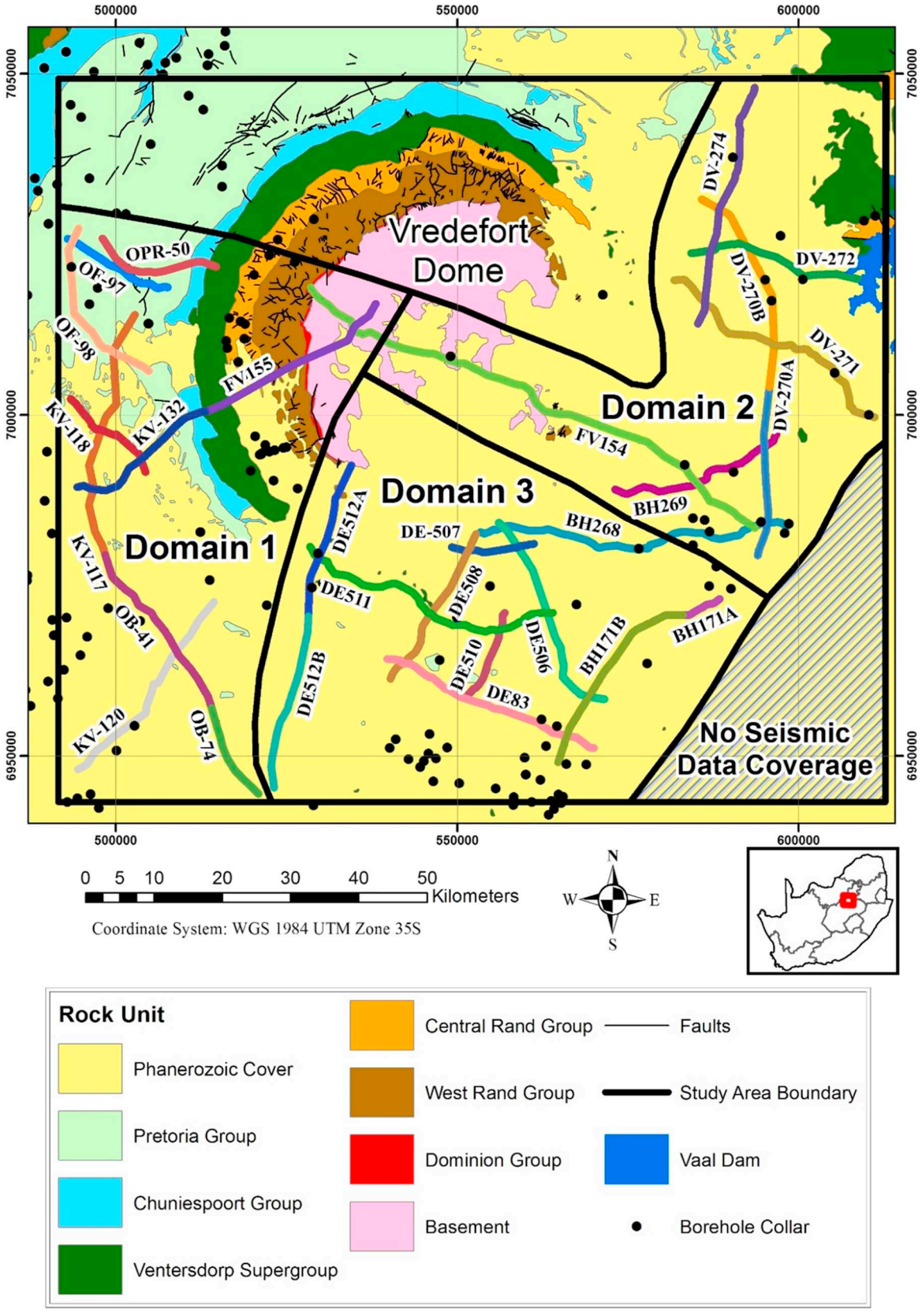

Fig. 4. Twenty eight 2D seismic lines (including three split lines) and boreholes overlaying 1:250,000 scale geology map. The three domains are illustrated and each contains a number of cross-cutting seismic lines.

Table 1
Published P-wave velocities (V_p) and bulk densities (ρ) for stratigraphy encountered in the study area.

Stratigraphic unit	Rock type	P-wave velocity (m/s)	Bulk density (g/cm^3)	Reflection coefficient	Reference
Karoo Supergroup	Various interlayered sediments (mudstone, sandstone, tillite)	3200[2] 3195[1] 3000[3]	2.38 (sandstone)[4] 2.54 (mudstone)[4]		[1]Pretorius et al., 1987; [2]De Wet and Hall, 1994; [3]Weder, 1994; [4]Jones, 2003
Hekpoort Formation	Volcanic (basaltic andesites and pyroclastics)	6083[1]	2.83[4]	+0.336[1] −0.068[1]	[1]Pretorius et al., 1987 [1]Pretorius et al., 1987; [4]Jones, 2003
Timeball Hill Formation	Shale dominated (minor quartzite, volcanics and diamictites)	5513[1]	2.80 (shale)[4] 2.67 (quartzite)[4]	+0.143[1]	[1]Pretorius et al., 1987 [1]Pretorius et al., 1987; [4]Jones, 2003
Malmani Subgroup	Dolomite (minor chert)	6834[1] 6600[3]	2.84 (dolomite)[4] 2.65 (chert)[4] 2.71 (shale)[4]	−0.061[1]	[1]Pretorius et al., 1987 [1]Pretorius et al., 1987; [3]Weder, 1994; [4]Jones, 2003
Pniel Sequence[a]	Allanridge Formation = quartzite, greywacke Bothaville Formation = mafic volcanics	6159[1]	2.84 (volcanics)[4] 2.70 (quartzite)[4] 2.76 (shale)[4]	−0.028[1]	[1]Pretorius et al., 1987 [1]Pretorius et al., 1987; [4]Jones, 2003
Platberg Group	Various interlayered sedimentary and volcanisedimentary units (shales, quartzite, conglomerate, mafic to felsic volcanics)	5827[1]	2.81 (volcanics)[4] 2.73 (quartzite)[4] 2.80 (shale)[4]	+0.033[1]	[1]Pretorius et al., 1987 [1]Pretorius et al., 1987; [4]Jones, 2003
Klipriviersberg Group	Mafic volcanics	6400[2] 6300[3] 6230[1]	2.88 (volcanics)[4] 2.90 (volcanics)[5]	−0.065[1]	[1]Pretorius et al., 1987 [1]Pretorius et al., 1987; [2]De Wet and Hall, 1994; [3]Weder, 1994; [4]Jones, 2003; [5]Manzi et al., 2014
Central Rand Group	Quartzite and conglomerate (minor shales and rare volcanics)	5779[1] 5750[2] 5550[3]	2.69 (quartzite/conglom)[4] 2.67 (quartzite)[5] 2.66–2.87 (quartzite)[6] 2.79 (shale)[4]	+0.025[1]	[1]Pretorius et al., 1987 [1]Pretorius et al., 1987; [2]De Wet and Hall, 1994; [3]Weder, 1994; [4]Jones, 2003; [5]Manzi et al., 2014; [6]Nkosi et al., 2017
West Rand Group	Various interlayered sediments (magnetic and non-magnetic shale, quartzite, conglomerate, minor diamictite and rare volcanics)	5748[1]	2.70 (quartzite)[4] 2.87–3.15 (shale)[6,b]	−0.018	[1]Pretorius et al., 1987 [1]Pretorius et al., 1987; [4]Jones, 2003; [6]Nkosi et al., 2017
Dominion Group	Tholeiitic andesite (minor quartzite, conglomerate)	~6000[c]	2.78 (volcanics)[4]	−0.012	This study [4]Jones, 2003
Basement	Granitoid	5693[1]	2.86[7]		This study [1]Pretorius et al., 1987; [7]Niu and James, 2002

[a] The Pniel Sequence is not recognised by SACS and therefore the Bothaville and Allanridge Formations that constitute it are standalone formations (Johnson et al., 2006).
[b] The shale density measurements of Nkosi et al. (2017) have been used to estimate the density range of the West Rand Group shales.
[c] The Dominion Group P-wave velocity was estimated with reference to the comparable rock types/bulk densities of the Hekpoort Formation and Klipriviersberg Group.

*V*1 and ρ1 are the V_p and ρ values for medium 1 respectively.
*V*2 and ρ2 are the V_p and ρ values for medium 2 respectively.

Seismic horizons are defined as surfaces, or reflectors that the seismic interpreter selects for picking based on their lateral continuity and strong seismic amplitudes. They are either picked as a trough or peak in the amplitude-based interpretation, depending on the polarity of the data. The amplitude display shows the changes in seismic acoustic impedance and thus helps to identify changes in lithological characteristics in the data. Borehole information is crucial in constraining the initial stages of picking. In the absence of borehole controls, a reasonable estimate based on experience and literature can be made. Interpretation of the data was divided into three domains, each containing numerous cross-cutting reflection seismic profiles and links to adjacent domains. The domains are illustrated in Fig. 4. The interpreted seismic reflectors, and their associated physical properties (V_p and ρ), corresponding to the main stratigraphic boundaries are given in Table 1.

In the 1980s, the Gold Division of the Anglo-American Corporation (AAC) (now known as AngloGold Ashanti) acquired approximately 16,000 km of 2D reflection seismic data across the Kaapvaal Craton for gold/platinum exploration and deep crustal studies (Pretorius et al., 2003). This extensive seismic program was followed by more than ten 3D reflection seismic surveys from 1990s to 2000s. The objectives of the surveys around the Vredefort Dome were to (1) delineate the overall extent of the gold-bearing horizons, (2) study the seismic response of the deformed rocks, (3) search for indications of new and extensions of gold deposits, and (4) extract structural information at depth. This study only focuses on twenty-eight of these 2D reflection seismic profiles that fall within the vicinity of the Vredefort Dome (Fig. 4).

Further details on the seismic design, acquisition and processing of these 2D seismic profiles are reported by Pretorius et al. (2003) and Molezzi (2017). The 2D reflection surveys were conducted and processed through the standard acquisition and processing parameters by the AAC processing team (see Pretorius et al., 2003). The parameters for each 2D reflection seismic acquisition are summarised by Molezzi (2017). The acquisition for all twenty-eight surveys, conducted by a CGG crew (Compagnie Générale de Géophysique), took place between 1985 and 1989. Each survey was designed to overlap with the survey line grids for comparison purposes. The surveys were recorded with a vibroseis source, spaced 50 m apart, using a fleet of two vibrators (Mertz M18) and 10 Hz geophones (spaced every 7.5 m or 4 m). The key

processing steps of the data included geometry update, trace editing, gain recovery, minimum phase conversion of the data, linear noise removal, first-break picking, refraction and residual static corrections, velocity analysis, muting, Normal-Moveout Correction (NMO) and stacking. Subsequent processing steps on the stacked data included deconvolution, amplitude equalization, and Kirchhoff or Finite difference time migration.

V_p and ρ data from borehole sonic logs of the Witwatersrand Basin goldfields (located outside the study area) is presented in Table 1. The data suggest a relatively large V_p and ρ variations from the quartzite units (V_p ~5200 m/s; ρ ~2.67 g/cm^3) of the Witwatersrand Supergroup to the dolomite units (V_p ~6800 m/s; ρ ~2.84 g/cm^3) of the Transvaal Supergroup (Pretorius et al., 2003; Manzi et al., 2012b). There were no downhole geophysical surveys (sonic and density logs) on the boreholes drilled in the study area to provide information about the acoustic impedances of the gold-bearing rocks and the associated lithological units; so the velocity used for time-to-depth conversion was obtained from the literature of historic vertical seismic profiling (VSP), 2D and 3D seismic surveys for the basin (Pretorius et al., 1994, 2000; Manzi et al., 2012a, 2012b). Time-to-depth conversion of the seismic sections was carried out using the constant velocity of 6000 m/s, providing a relatively good correlation between strong seismic reflections and borehole data. The depth locations of the stratigraphy obtained from these seismic sections agreed with those reported by Pretorius et al. (1994), Friese et al. (1995), Tinker et al. (2002), and Manzi et al. (2012b).

3.1.3. Borehole information

In total 208 borehole lithology logs acquired from the Council for Geosciences (CGS) were captured and used to constrain the seismic interpretation and geological modelling. To optimise the data capturing process, boreholes in close proximity to the 2D reflection seismic profiles were prioritised to constrain the seismic interpretations at depth. Of the 208 boreholes, only 46 were priority and the remaining 162 were used as infill data for the geological model.

3.2. Phase 2: interpretation of 2D seismic sections

For the sweep of 10–91 Hz, as reported by Pretorius et al. (2003) for these seismic surveys, the dominant frequency observed during processing of the seismic data was about 65 Hz (Pretorius et al., 2003). Based on the Rayleigh quarter of dominant-wavelength criterion described by Widess (1973), and by using the average V_p of 6000 m/s obtained during processing (Manzi et al., 2012b), the vertical resolution is about 23 m. This implies that the beds (or layers) with thickness less than 23 m cannot be vertically resolved in these seismic sections, however, features below this limit can be detected (Manzi et al., 2014). Using the Fresnel zone criterion, after migration, the horizontal resolution is equivalent to the dominant wavelength, which is approximately 92 m. Using this criterion, first-order scale faults, as defined by Manzi et al. (2013) for the goldfields, were relatively easy to identify and picked on seismic sections (faults with a throw of 400 m to 2500 m).

The variation in rock types in the study area ranges between clastic sediments, dolomite and volcanic rocks. V_p and ρ values for quartzite and shale, including their protoliths (i.e. sandstone and silt/mudstone) differ slightly, but the values are reasonably comparable to one another. The V_p and ρ values of the weakly metamorphosed sandstone and mudstone of the Karoo Supergroup differ by 200 m/s and 0.16 g/cm^3, respectively. However, according to Phillips and Law (1994) the regional metamorphic grade of the Witwatersrand Basin (outside the collar of the dome) is lower greenschist facies (i.e. temperatures up to 400 °C, and pressures up to 3 kb). The V_p and ρ values of these lower greenschist facies quartzite and shale units in the study area differ comparably to Karoo Supergroup sedimentary rocks. These values are ~2500 m/s and ~0.3 g/cm^3 higher for both quartzites and shales, compared to the Karoo Supergroup (Table 1).

Importantly, mudstones and shales are generally denser than sandstones and quartzites. The significant variations in the V_p and ρ values would result in acoustic impedance contrasts that would produce a seismic reflection at the interface. On the other hand, dolomite ρ values change very little at lower greenschist facies (2.84 g/cm^3 in the metamorphosed Malmani Subgroup versus 2.86 g/cm^3 in un-metamorphosed rocks; Jones, 2003). Similarly, all volcanic units exhibit V_p and ρ values above 6000 m/s and 2.78 g/cm^3, respectively. Therefore, reflections observed on seismic sections are due to a significant acoustic impedance contrasts at the interfaces between the various mediums (i.e., volcanic rocks, quartzites, shales, and dolomite).

The 2D seismic sections were used to interpret seven major lithological contacts for the modelling phase. The interpretations of the 2D reflection seismic profiles were made dynamically. Upon completion of the initial interpretation each section was systematically added to the 3D workspace of Leapfrog Geo®. These interpretations were then modified multiple times over as new interpreted sections were added to the 3D workspace. This ensured that continuity of the seismic reflections became increasingly refined.

Horizons picked (i.e. picking strong reflectors) in the 2D reflection seismic sections corresponded with horizons digitised from surface mapping so that surface to depth wireframe-supports could be created. The quality of the seismic data (i.e. identifying the stability and continuity of the strong reflections) was evaluated in Kingdom Suite® interpretation software package. However, due to the software modelling limitations, horizons were picked and interpreted in ArcGIS®, then imported into LeapFrog Geo® and digitised directly in the software.

3.3. Phase 3: digitising

Borehole data were efficiently used as constraints in the interactive 3D workspace of Leapfrog Geo® because of the categorised information captured from the logs. Surface geology maps were incorporated in Leapfrog Geo® to provide additional constraints on the interpretation. Further to this, the interpretation of each seismic section from the various data sources was created in ArcGIS®, and the images were imported into LeapFrog Geo® as vertical sections. Each vertical section was draped onto corresponding vertical seismic section meshes (which were created from the geometry data of the individual seismic surveys).

3.4. Phase 4: geomodelling

The 90 m resolution SRTM elevation model was used to create the topographic surface of the study area in LeapFrog Geo®. The model required a 3D block boundary to confine the limits of the interpolations (mathematical links/extrapolations between data points that combine to create the 3D surfaces). The topography bounded the upper z-axis limit, and the 2D seismic profiles bounded the x, y, and lower z-axis limits. The boundary cube was extended by a few kilometres to allow a small amount of additional interpolation beyond the outermost 2D seismic profiles. The z-axis boundary base was set to the depth extent of the seismic sections (i.e. ~20 km, including ~2 km of additional interpolation below the sections).

Eight geological volumes were created for the 3D model using the seven major interpreted lithological contacts (i.e. seismic horizons). The volumes were generated in LeapFrog Geo® using its implicit modelling algorithm (named FastRBF™) based on geochronological order. A wedge in the southeast of the study area contained no data and was removed from the geological model.

Geological model volumes were defined by wireframes. Volumes were created using the interpreted wireframes of the digitised contact horizons, as well as additional support wireframes (polylines and orientation disks) that provided lateral constraints to the interpolations between the seismic lines.

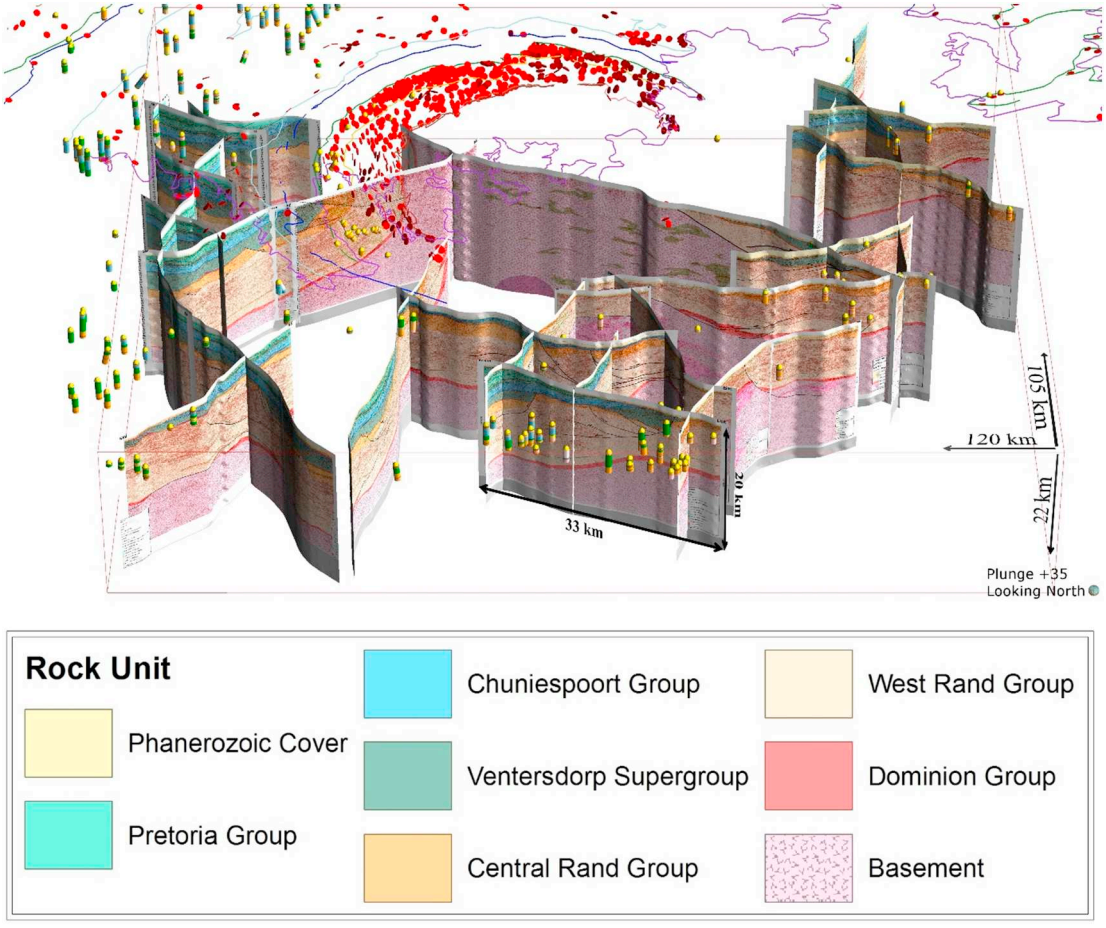

Fig. 5. 3D view looking north, plunging at 35°, combined seismic interpretations, boreholes, and digitised surface mapping data. Seismic section interpretations have been made transparent to show the underlying reflections. Surface mapping contacts between the various rock units are illustrated as polylines. Key: Purple = Phanerozoic/Karoo Supergroup base contact; light blue = contact Pretoria – Chuniespoort groups; dark blue = Black Reef Formation; Green = VCF; Yellow = contact Central Rand – West Rand groups; brown = contact West Rand – Dominion groups; dark red = contact Dominion Group – Basement; pink = contact Basement – Other; Red orientation disks = Surface structural data. Note, the yellow markers at the top of each borehole are collar markers. (For interpretation of the references to colour in this figure legend, the reader is referred to the web version of this article.)

4. Results

4.1. 2D seismic section interpretations

The seismic sections shown in Figs. 5–8 (together with constraining surface and borehole data) are characterised by strong seismic reflections across the study area from ~200 m to ~22 km depths due to significant acoustic impedance contrasts at the geological interfaces. The major stratigraphic units delineated in the seismic sections include the Karoo, Transvaal, Ventersdorp and Witwatersrand supergroups, as well as the Dominion Group and basement TTG suite. Seismic data also show imaging of major unconformities across all three domains, i.e., at the contact of the Venterspost Contact Formation (VCF) with the Central Rand Group, and the Black Reef Formation against all older stratigraphic units. Progressive termination of the major supergroups against the Karoo Supergroup is detected in the east of the study area. Further detailed interpretation of the seismic sections for Domains 1, 2, and 3 is provided by Molezzi (2017).

Two fold systems are imaged in Domain 1, however the relative timing between the two systems is unclear from the 2D seismic sections. The first fold system (FS1) is illustrated in Fig. 6a, and includes macroscopic upright open folds imaged in the Transvaal Supergroup with wavelengths of ~16 km and amplitudes of ~350 m. The axial planes are subvertical and trend northeast (~050°). The second fold system (FS2) is illustrated in Fig. 6b and comprises an asymmetric syncline that borders the Vredefort Dome, with an axial plane that dips towards the dome (possibly associated with the central uplift). The axial plane orientations of FS1 are oblique to the asymmetric syncline of FS2, and therefore associate poorly with the deformation related to the central uplift. FS1 in the seismic sections concur with observations by Simpson (1978) for the Pretoria Group. The folds adjacent to the dome exhibit decreased wavelengths, down to ~5 km and increased amplitudes, up to ~600 m.

A well-developed listric fault system is interpreted in the southern half of Domain 1 with fault offsets up to 1 km, as illustrated in Fig. 7. The basal plane of the listric fault system traces across seismic profiles (e.g. KV-120, OB-41, and OB-74). The VCF interface exhibits a strong seismic reflection as result of an unconformable contact with the underlying stratigraphy. However, the offsets of the interface are observed across the listric fault system. The extent of the offsets into the Ventersdorp Supergroup is unknown because the package is seismically transparent. In addition, a low-angle fault extends into the lower West Rand Group, adjacent to the interface of Dominion Group with the basement. Several other offsets are identified and interpreted in the seismic sections. These include listric fault offsets of the VCF in Domains 2 and 3, and at the interface between the West Rand and Central Rand groups in Domain 2.

In Domain 2, the Transvaal Supergroup is only interpreted on seismic sections in the northern half of the domain. The southern half of the domain is uplifted by ~4 km. A large anticlinal fold is interpreted in

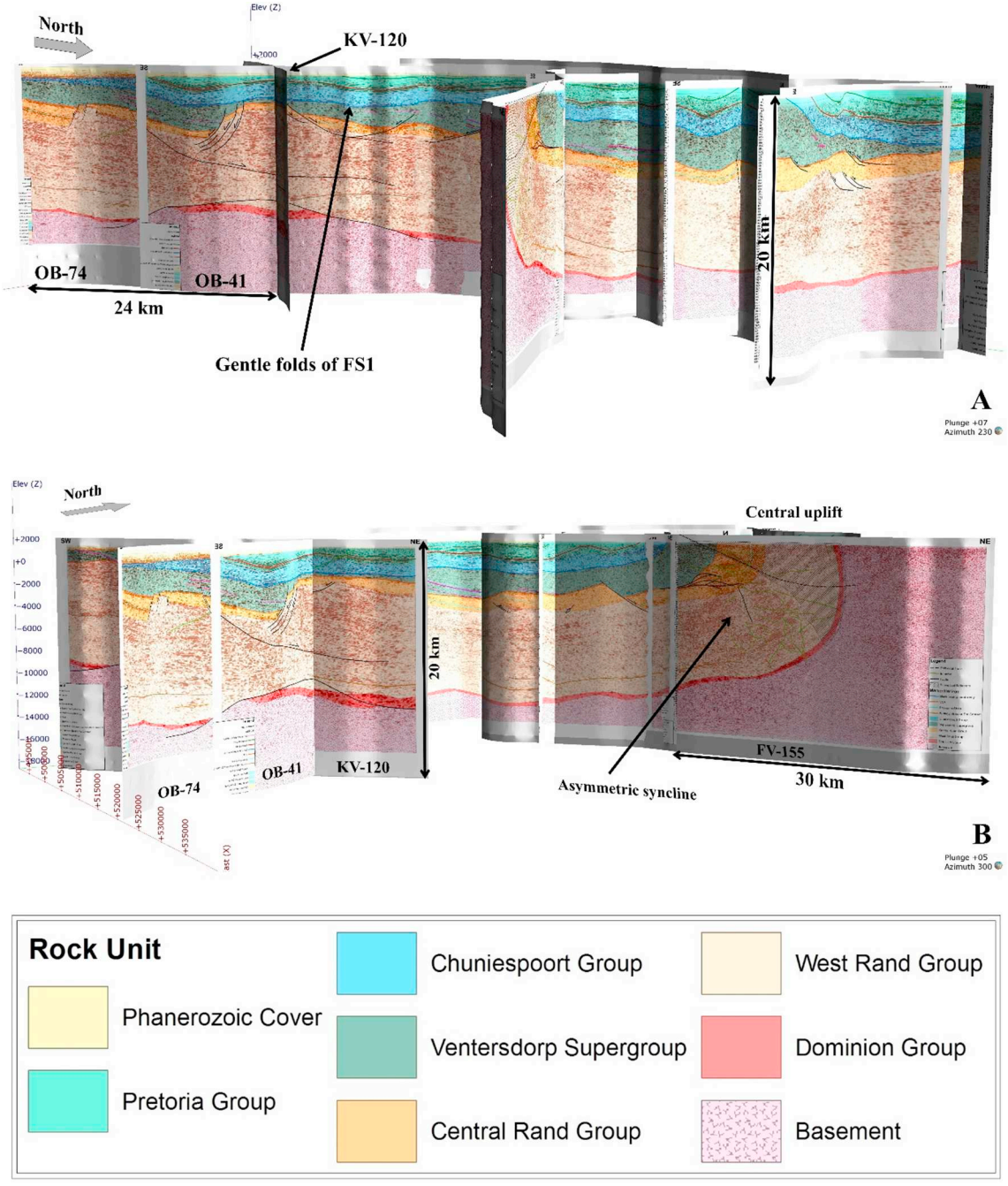

Fig. 6. Two 3D views of the eight interpreted seismic lines in Domain 1. Note, the plunge angles were used to provide perspective, and do not form part of any structural interpretations. A) Looking towards 230° plunging at 07°, displaying gentle folds of FS1. B) Looking towards 300° plunging at 05°, highlighting FS2, an asymmetric syncline related to the central uplift.

the east in Domain 2 and is illustrated in Fig. 8. The fold is seismically imaged and distinct in several seismic profiles, i.e. DV-270A/B, DV-271, DV-272, and DV-274, and exhibits an axial plane that trends 035° (viewing direction of Fig. 8a). The southern limb of the fold is crosscut and offset by a large listric fault. The estimated trend of the fault is 100° (viewing direction of Fig. 8b), which differs from the axial plane of the anticline by 65° (i.e. 100° versus 035°).

In Domain 3, the orientations of the seismic reflections shift from upright, steeply dipping units in the west of the dome to upright, shallow dipping units in the east. The interface of the basement is also elevated in the east, coinciding with the elevated strata observed in the adjacent portion of Domain 2.

4.2. 3D geological modelling

The creation of the 3D geological model represented the final phase of the modelling framework (Fig. 3). The final volumes provide adequate representation of the regional scale architecture in the study area. The spatial relationships also provide insight into the formation and preservation of major stratigraphic units. These volumes are separated by seven major stratigraphic boundaries (see Fig. 2). The methodology for digitising datasets to form the wireframes of the individual 3D geological volumes and subsequent creation of the 3D geological model have been described and discussed by Molezzi (2017). The final geological model is displayed in Fig. 9.

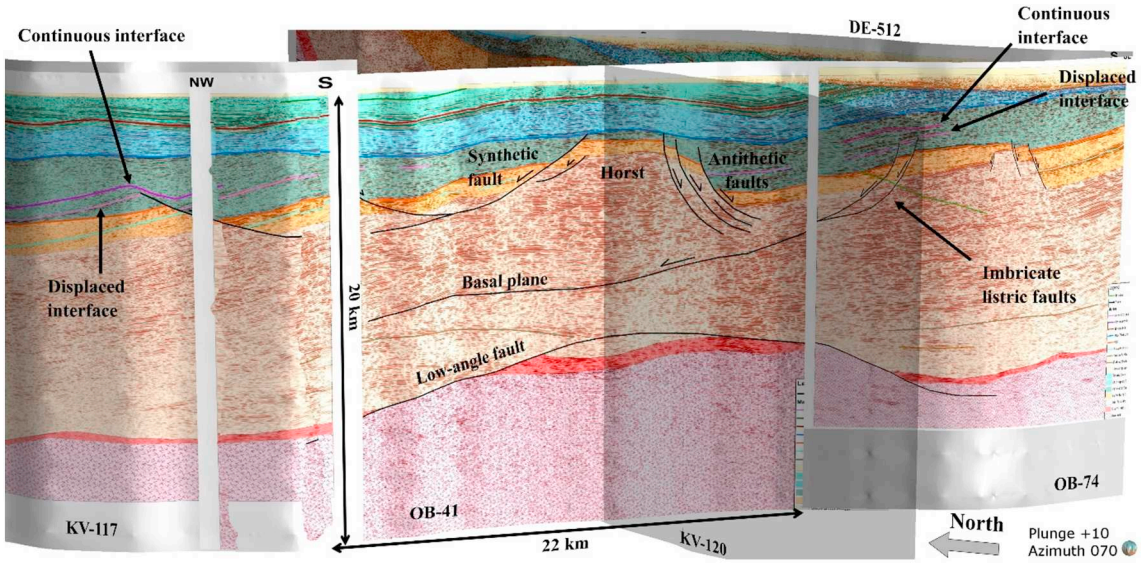

Fig. 7. Well-developed listric fault system imaged in the southern half of Domain 1. Timing is constrained to post-Klipriviersberg Group and syn-Platberg Group. The structures were also imaged in seismic section KV-120, but it was made transparent for unobstructed clarity of the system. Viewing direction is towards 070° and plunging 10°.

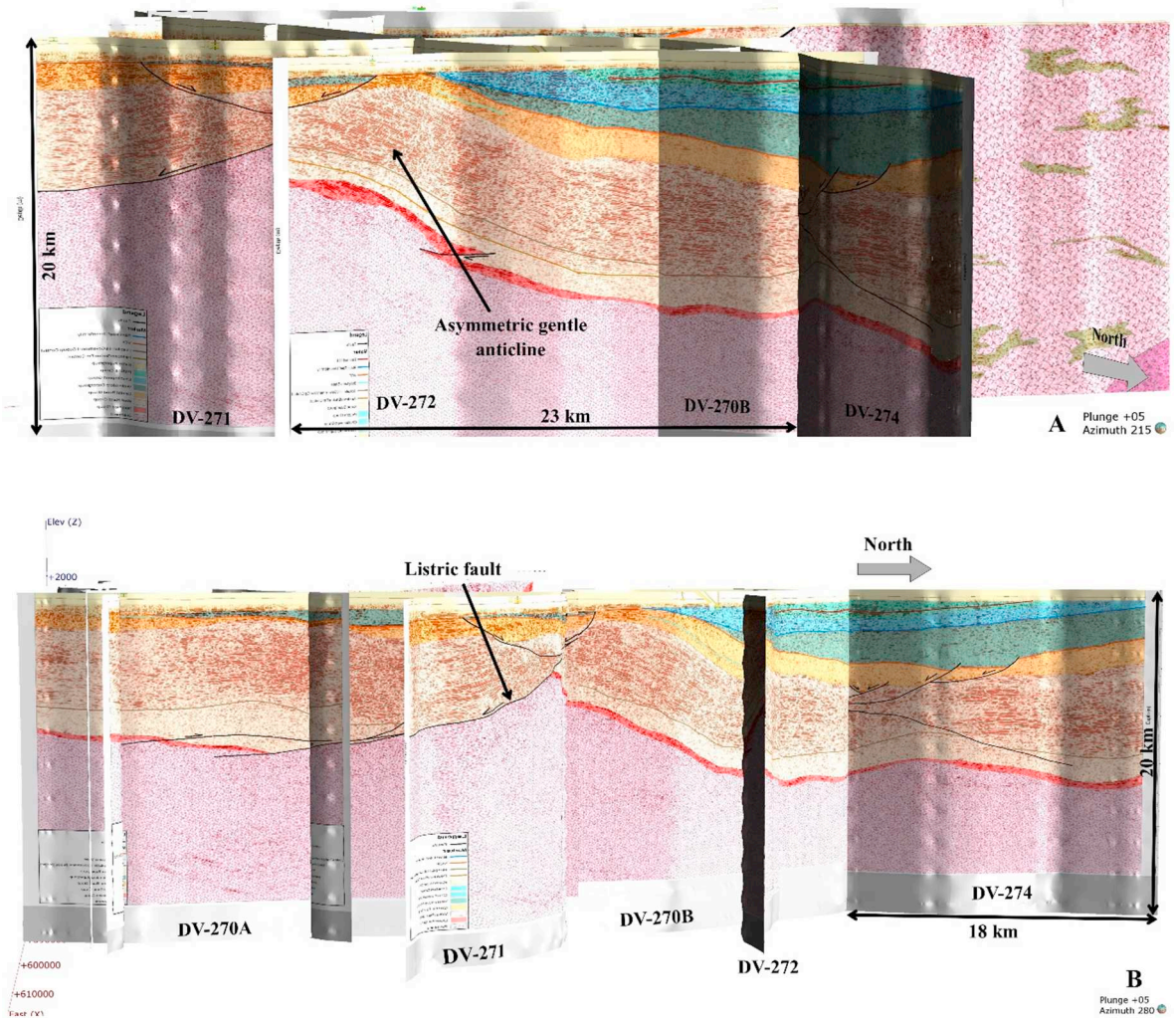

Fig. 8. Two 3D views of the eight interpreted seismic lines in Domain 2. Note, the plunge angles were used to provide perspective, and do not form part of any structural interpretations. A) Looking towards 215° plunging at 05°, along the axial plane trend of the large anticlinal fold. B) Looking towards 280° plunging at 05°, along strike of the listric fault that crosscuts and offsets the anticlinal fold.

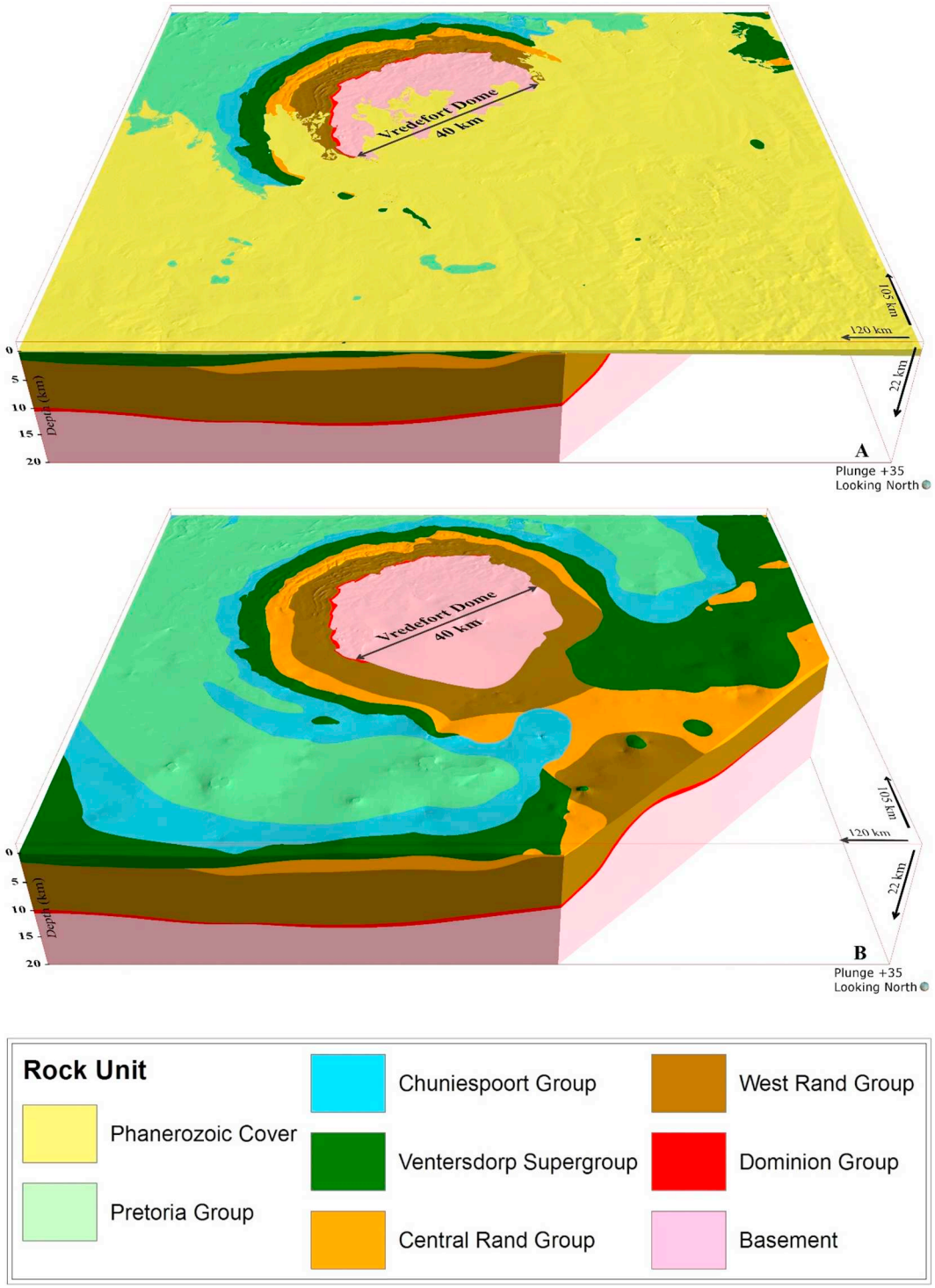

Fig. 9. Eight modelled volumes. A) Model including the Phanerozoic/Karoo Supergroup cover. B) Model excluding the Phanerozoic/Karoo Supergroup cover.

5. Discussion

5.1. Central Rand Group volume

The output volume for the Central Rand Group is displayed in Fig. 10. The underlying West Rand Group exhibits a series of closely-spaced, contiguous internal seismic reflections associated with the large variation in V_p and ρ of the layered sedimentary package. However, the Booysens Formation of the Central Rand Group is poorly detected across the study area; the shales of Kimberley Formation and the Bird Lava Member of the Krugersdorp Formation are not reported in boreholes or surface maps inside the study area. The quartzite and conglomerate units that make up the Group exhibit comparable V_p and ρ (Table 1). Therefore, in contrast to the West Rand Group, the Central Rand Group is defined as a seismically transparent package throughout the study area.

The view in Fig. 10 illustrates the regional-scale erosional surface of the VCF which forms the upper contact of the Central Rand Group. In four areas (marked by the "X" in Fig. 10) the VCF overlies the West Rand Group. These anomalies indicate local exposure of the West Rand

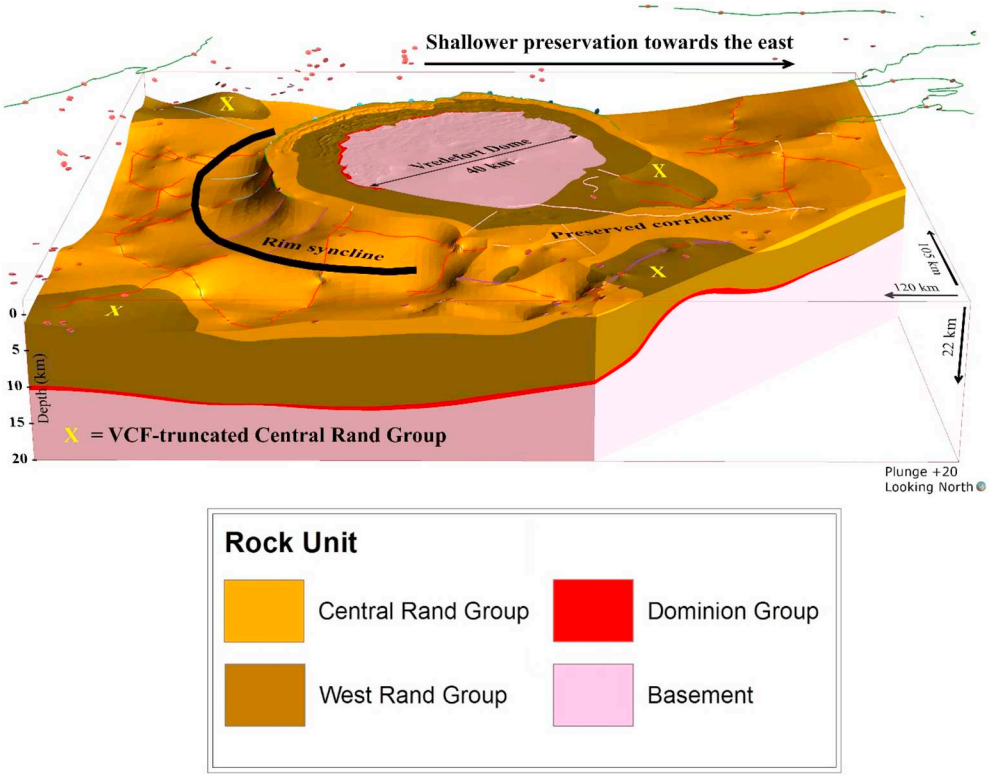

Fig. 10. Modelled volume of the Central Rand Group, including chronologically older units. Dark blue polylines represent the structure-defined contacts; red polylines represent the unconformable lithological contacts; green polylines represent the surface contacts; purple, pink and light blue polylines represent support wireframes. (For interpretation of the references to colour in this figure legend, the reader is referred to the web version of this article.)

Group by erosion prior or synchronous to deposition of the VCF. This conclusion is also supported by adjacent borehole data.

The Central Rand Group is preserved in a narrow corridor in the southeast. The corridor lies between two zones of elevated basement, one associated with the Vredefort Dome, the other with a relatively smaller discrete uplift. The rim syncline (FS2) is observed only on the western margin of the dome. The equivalent stratigraphic units on the eastern margin are preserved several kilometres higher up in the crustal package. They also exhibit variable architecture compared to the west (which is dominated by the rim syncline). The Central Rand Group on the northwest and southwest margins of the dome, as well as the southern margin of the model boundary is elevated. These areas form the distal parts of the rim syncline and, as the modelling illustrates, suggests that the rim syncline continues eastwards into Domain 3, beneath the Phanerozoic cover (see Fig. 1 for reference).

5.2. Ventersdorp Supergroup volume

The output volume for the Ventersdorp Supergroup is displayed in Fig. 11. The upper surface of the volume represents the Black Reef Formation erosional unconformity. The Ventersdorp Supergroup is characterised as a seismically transparent package across most of the study area due to the dominance of mafic volcanic compositions. Although both the Central Rand Group and Ventersdorp Supergroup are transparent the interface is detected due to the acoustic impedance contrast produced by the change in V_p and ρ across the contact between the two units (Table 1).

The Ventersdorp Supergroup volume is elevated in several places. These include the northwest corner, southwest corner, eastern margin of the model boundary, and across the southeast. Except for the southeast elevation, these areas possibly form part of the rim syncline around the dome. The elevated Supergroup in the southwest corner of the model boundary comes to contact with an elevated West Rand Group volume. Borehole data in this area record truncation of the Platberg Group by the younger Bothaville and Allanridge formations, and deposition of these formations over the Klipriviersberg Group, suggesting at least two episodes of uplift.

On the northwest margin of the modelled block the Ventersdorp Supergroup is truncated by the Black Reef Formation across a narrow area. An additional truncation is imaged in seismic sections in the east, and reported in boreholes, towards the hinge of the interpreted anticline. Across the hinge of the anticline, the Ventersdorp Supergroup is absent because the Karoo Supergroup unconformably overlies the Central Rand Group.

Towards the southeast (marked by the “X” in Fig. 11) the Ventersdorp Supergroup is absent across a large portion of the volume. This anomaly is based on borehole information, surface mapping, and seismic section interpretations. These indicate that the Karoo Supergroup unconformably overlies the Witwatersrand Supergroup. Surface mapping and borehole information reported a few narrow volcanic outcrops and intersections of the Klipriviersberg Group near the southeast margin of the modelled block. These constraints indicate that the uplift in the southeast of the model boundary formed prior to or synchronous with emplacement of the Klipriviersberg Group.

A couple of periclinal folds exposed around the dome are the result of integrating the surface mapping and 2D seismic data. Unfortunately, the relative timing of these periclinal folds cannot be ascertained using the available datasets because detailed structural information from outcrop analyses was not available in this study. One of these folds is observed to the west of the dome and coincides with the surface expression ~2.8 km above it. Another periclinal fold is located adjacent to the southwest margin of the dome where it is covered by Phanerozoic sedimentary rocks. The slightly arcuate strike of the subvertical axial plane trends eastwards towards the dome, forming an acute angle with the margin of the dome. The fold and its arcuate axial trace are better represented in the overlying Chuniespoort Group volume (Fig. 12).

5.3. Chuniespoort Group volume

The output volume for the Chuniespoort Group is displayed in Fig. 12. In the study area the Penge Formation ironstone is not preserved according to surface mapping and boreholes. The Duitschland

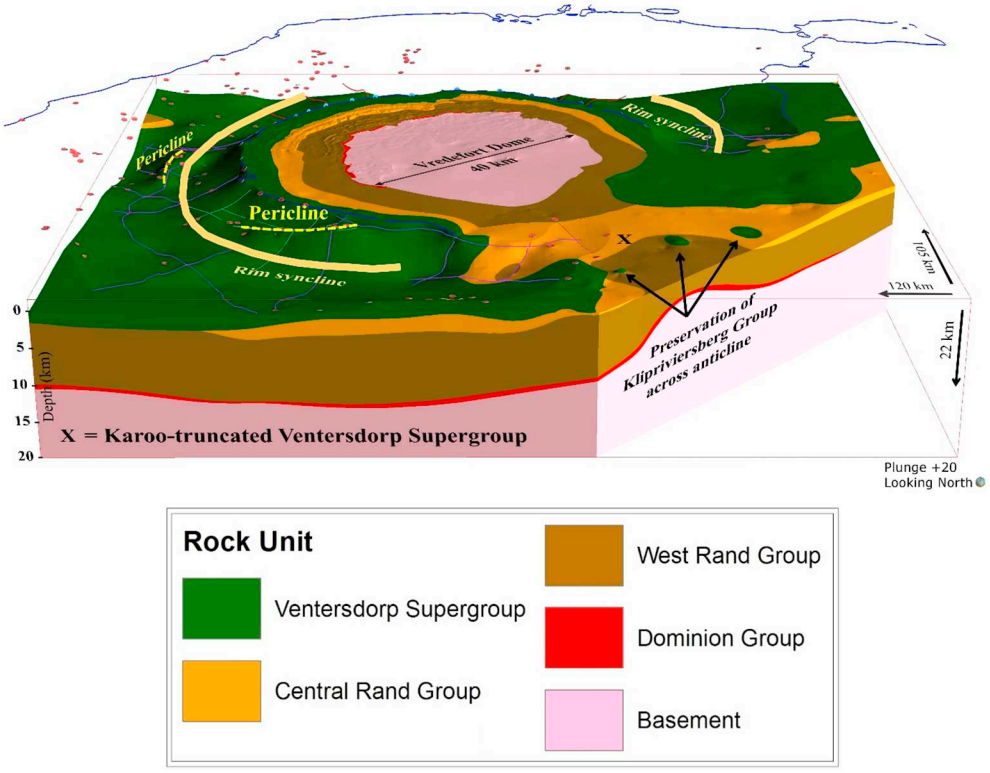

Fig. 11. Modelled volume of the Ventersdorp Supergroup. Purple polylines represent the unconformable lithological contacts; blue polylines represent the surface contacts; grey-green and red polylines represent support wireframes. (For interpretation of the references to colour in this figure legend, the reader is referred to the web version of this article.)

Formation is not explicitly reported either, but due to the absence of the Penge Formation, the carbonates that dominate this formation (Johnson et al., 2006) may be merged in the borehole logs with the underlying Malmani Subgroup dolomites. For example, the borehole logs in the southern parts of the study area do not differentiate the various carbonate intervals. The Malmani Subgroup exhibits discrete, discontinuous low-amplitude internal seismic reflections. However, the dolomite sequences dominate the subgroup to produce the relatively high V_p of the subgroup (6600–6834 m/s). Therefore, the seismic character of the subgroup differs from the overlying Timeball Hill Formation of the Pretoria Group, and enabled robust imaging of the contact.

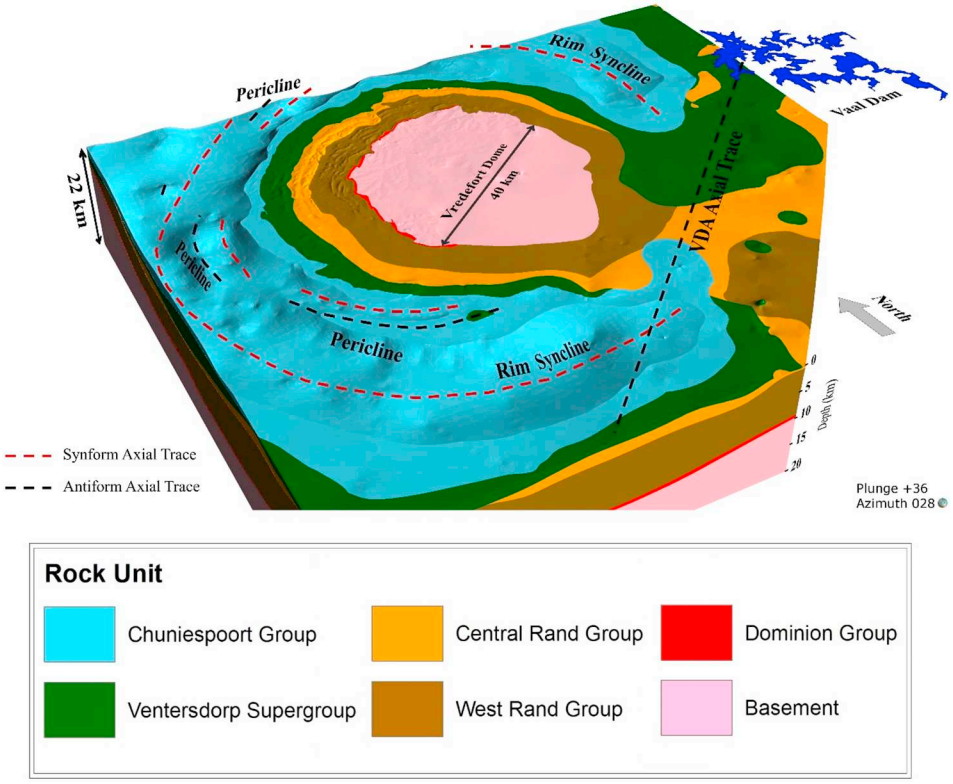

Fig. 12. Geological model highlighting axial traces imaged on the contact between the Chuniespoort and Pretoria groups (i.e. the Pretoria Group volume was omitted from the view to show the contact surface). The proposed periclinal folds are preserved in the rim syncline around the dome. The Vaal Dam is included as reference to the VDA axial trace being sub-parallel to the elongate northern section of the dam. View orientation is towards 028°, plunging 36°.

The Chuniespoort Group is confined in the south, southeast, and east. The Group on the southern and eastern margins of the modelled block exhibits dome-dipping orientations, conforming to the geometry of the rim syncline around the dome. However, the synclinal geometry is absent in the southeast. Interestingly, in relation to the absent corridor observed in the underlying Ventersdorp Supergroup, southeast of the dome, the Chuniespoort Group exhibits an absent corridor further north. For reference, the axial trace of the imaged anticline in the east is included together with the Vaal Dam. This is a reference to the association between the axial plane trend and the broad, elongated northern section of the dam.

The periclinal folds exposed in outcrops of the Pretoria Group and located west and north of the dome are expressed at depth in the Chuniespoort Group volume (as well as the Ventersdorp Supergroup volume discussed above). An additional periclinal fold is interpreted using borehole intersections and seismic sections and is located beneath the Phanerozoic cover adjacent to the southwest margin of the dome. The fold axial trace trends acutely towards the southeast margin of the dome. However, the Chuniespoort Group volume better defines the convergence of the fold with the collar rocks. The crest of the periclinal fold may be located near the narrow outcrop position of the exposed Klipriviersberg Group; possibly slightly west of it in account of the proximity to the repeated group in the adjacent collar rocks.

5.4. Strato-structural features

The integration and interpretation of datasets in 3D space provided insight into the strato-tectonic architecture of the area surrounding the Vredefort Dome. There are numerous model-scale strato-structural features that are interpreted and constrained in the seismic sections. These are illustrated in Fig. 13 and are presented below in chronological order. A summary of examples is presented in Table 2.

Feature 1: A normal fault is interpreted in the modelled dataset and imaged in seismic section BH-268 in Domain 2. It exhibits normal offset of reflections in the Dominion Group and the lower West Rand Group. It has a calculated apparent throw of ~700 m in the plane of the sections. The reflections in the lower West Rand Group are conformable across all three domains, i.e. there is no evidence of inclined reflections that terminate against distinct interfaces. The timing of this fault is constrained by the offset of reflectors to syn-lower West Rand Group deposition but cannot be associated with any specific formation.

Feature 2: This feature relates to the interface between the West Rand and Central Rand groups. In some seismic sections the undulate erosional contact between the groups exhibits an apparent normal offset of approximately 400–500 m in the plane of the seismic sections. These are seismically imaged and shown in seismic sections OF-97 and OPR-50. A 3D projection of these faults reveals a trend of 032°and dips of 45° to 55°.

Feature 3: This feature relates to the VCF interface. The two areas in the east of the modelled volume exhibit truncation of older units against the VCF, i.e. an unconformity is interpreted. In the northwest and southwest of the modelled volume the borehole data reports Platberg Group metasedimentary rocks unconformably overlying the Witwatersrand Supergroup. However, the boreholes in the east report Klipriviersberg Group volcanic rocks unconformably overlying the Witwatersrand Supergroup. Therefore, the unconformity in the west is interpreted as younger and unrelated to those observed in the east.

Feature 4: This feature relates to the timing of the listric faults. The most well developed system is interpreted from several seismic sections in the southwest, as illustrated in Fig. 7. The timing of these structures is constrained by offsets of reflections in the otherwise seismically transparent Ventersdorp Supergroup (seismic sections KV-117 and OB-74).

The faults offset the lower reflection in both seismic sections (labelled as displaced interface in Fig. 7). The overlying reflection in seismic section OB-74 is continuous across the offset (labelled as continuous interface in Fig. 7). The comparable, overlying reflection in seismic section KV-117 is also continuous, but is conformable with the fault orientation across the offset. It is therefore interpreted that the lower reflection represents the interface between the volcanic rocks of the Klipriviersberg Group and the sedimentary rocks of the unconformably overlying Kameeldoorns Formation.

As summarised by Johnson et al. (2006), the Goedgenoeg Formation is characterised by the onset of volcanism that gradually cessed sedimentary deposition of the Kameeldoorns Formation. The change in V_p and ρ would produce a seismic reflection at the interface. Therefore, the second reflection is interpreted to represent the interface between the Kameeldoorns and Goedgenoeg formations. These observations assert an important aspect of the sequence boundary, that the formation of the listric fault system is constrained as post-Klipriviersberg Group and pre- to syn-Platberg Group, or extensional collapse at that time, i.e. between ca. 2.7 Ga and ca. 2.64 Ga. These observations concur with the Hlukana-Platberg Event proposed by Manzi et al. (2013).

Feature 5: This feature relates to the interface of the Black Reef Formation with older formations. The interface is the most prominent in the seismic sections. It is enhanced by the changes in reflection orientations across the interface, between the overlying conformable units and the older acutely oriented units. The interface represents an unconformity that forms the upper contact surface of the Ventersdorp Supergroup in a few outcrop locations in the study area. Boreholes and the seismic sections in the south and southeast indicate that the Black Reef Formation terminates against the Karoo Supergroup.

Feature 6: This feature relates to fold geometries of FS1 in the Transvaal Supergroup. The folds exhibit gentle, long wavelength, low amplitude characteristics, and are imaged across all three domains. The youngest unit of the Transvaal Supergroup in the study area is the Magaliesberg Formation. The unit forms part of FS1, therefore constraining fold formation to post-Magaliesberg Formation, at 2193 ± 20 Ma (Bumby et al., 2012).

The folds are pronounced in the west, whereas a single large, asymmetric, gentle, first-order scale anticline is interpreted in Domain 2 (described previously, in Fig. 8). This fold is hereafter referred to as the Vaal Dam Anticline (VDA). Importantly, the surface extent of the Vaal Dam reservoir indicates that the northern section of the reservoir lies adjacent to the hinge zone of the VDA and is elongated along the strike of the fold axial plane (~050°), as illustrated in Fig. 12. Although the folds exhibit different wavelengths and amplitudes, they have corresponding subvertical axial planes, with parasitic folds to the main anticline (Fig. 14).

Feature 7: The VDA in Domain 2 is crosscut by a listric fault that exhibits a rollover anticline in the hangingwall (Fig. 8). It is interpreted that listric fault development took place after the folding event described above.

5.5. Comparisons with published work

Several publications present structural features and deformation events that are relevant to the study area. These include interpretations of seismic sections (Friese et al., 1995; Tinker et al., 2002), and tectonic evolution in the study area (Friese et al., 1995; Henkel and Reimold, 1998; Johnson et al., 2006; Dankert and Hein, 2010; Manzi et al., 2013; Frimmel, 2014), including the late to post-Transvaal Supergroup folding event (Alexandre et al., 2006; Dankert and Hein, 2010). In consideration of the published tectonic evolution of the study area, and following the comparisons with this study, a combined tectonic history is presented in Fig. 15.

In terms of published seismic section interpretations, Tinker et al. (2002) presented an interpretation for the crosscutting seismic sections KV-117, OB-41, and OB-74 (termed by them as a single section, “OB”). Fig. 16 displays the interpretations from this study and the published version. The vertically exaggerated interpretation of Tinker et al. (2002) relied upon a single borehole, labelled “A” in the publication,

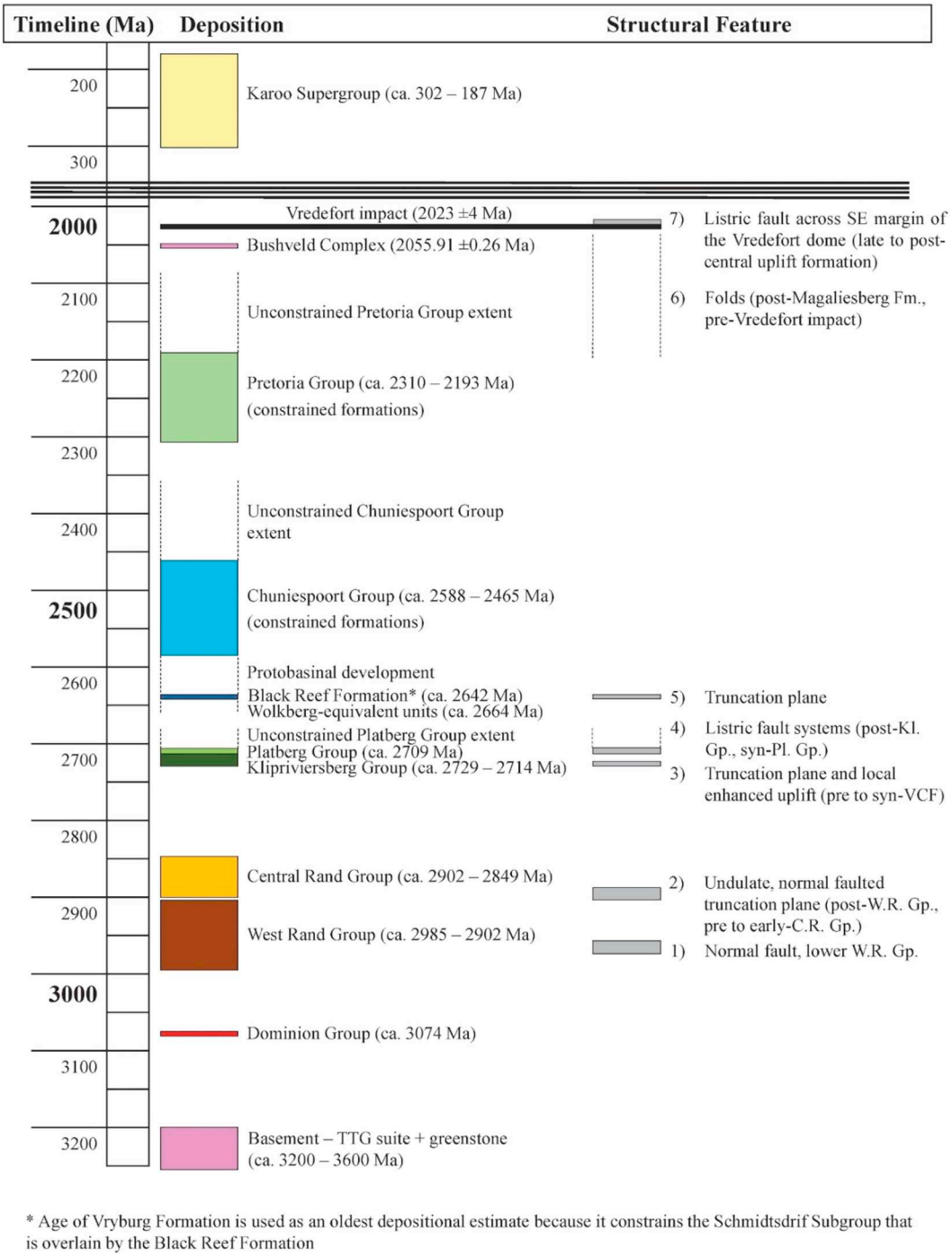

Fig. 13. Schematic chart highlighting the seven main structural features imaged in the study area. The stratigraphy has been included as a cross-reference to the estimated timing of the structures.

and an intersecting seismic section, termed "AG", as depth constraints. Borehole "A" and section "AG" are not part of the dataset in this study. For reference, seismic section KV-120 intersects section OB-41 adjacent to the collar position of borehole "A".

The published borehole coincides very well with the imaged units in seismic sections KV-120, OB-41, and OB-74. The interfaces and the structural features are similar in both interpretations, i.e. preservation of a large horst preserved between sets of normal faults, and folds in the Transvaal Supergroup. Overall, these two sections exhibit similar structural regimes, i.e. listric faults developed post-emplacement of the Klipriviersberg Group, erosion during the Black Reef Formation, and post-Hekpoort Formation folding.

Several 2D reflection seismic and gravity sections were re-interpreted by Friese et al. (1995) who produced a map of the Witwatersrand Basin superimposed with various structures. The interpretation includes a series of thrust faults that dominate the unexposed southeast. However, these thrusts were not imaged by the seismic method (Fig. 17). Reverse/thrust fault offsets of older rock over younger were also not observed. It is suggested that if the reverse/thrust faults do exist, they contain offsets that are too small to be detected with confidence in this study.

In comparison to the structural features discussed in Section 5.4, the interpretations concur with the literature as well as several published tectonic events (including Alexandre et al., 2006; Johnson et al., 2006;

Table 2
Summary of structural features and associated seismic section examples.

Structural feature		Example
1)	Normal offset of Dominion and West Rand groups	Offset in seismic section BH-268 in Domain 2
2)	Normal offset of undulating erosional contact between West Rand and Central Rand groups	Offsets in seismic sections OF-97 and OPR-50 in Domain 1
3)	Truncation of the Witwatersrand Supergroup by the Ventersdorp Supergroup	VCF truncation (seismic section KV-120 in Domain 1; FV-154, BH-269, and DV-270A in Domain 2; BH-171A/B in Domain 3)
4)	Listric fault systems, post-Klipriviersberg Group, syn-Platberg Group	Seismic sections KV-120, OB-41 and OB-74 in Domain 1 show a single system; DV-274 in Domain 2; DE-512B in Domain 3
5)	Truncation of older units by the Black Reef Formation	Examples throughout the study area, exhibited in most seismic sections.
6)	Gentle, long wavelength, low amplitude folds	More pronounced in all north-south trending seismic lines in Domain 1. A single large fold termed the Vaal Dam Anticline (VDA) is imaged in seismic sections DV-270B, DV-271, and DV-272 in Domain 2.
7)	Large listric fault displaces the VDA and extends at least 65 km across the southeastern margin of the Vredefort dome	Seismic sections BH-268, BH-269, FV-154, DV-270A (VDA displacement), and DV-271 (VDA displacement) in Domain 2; DE-506, DE-507, and DE-508 in Domain 3.

Dankert and Hein, 2010; Manzi et al., 2013; Frimmel, 2014). The interpretation of a tectonic event after the deposition of the West Rand Group and prior to deposition of the Central Rand Group (the Asazi Event of Manzi et al., 2013) is supported in the study area. This was because many seismic sections exhibited an undulate, erosional interface between the West Rand and Central Rand groups. The interface also includes several localised fault offsets, with the possibility that smaller scale offsets are more frequent.

Collisional tectonics reported by Johnson et al. (2006), Dankert and Hein (2010), and Frimmel (2014) and others, describe the closure of the Central Rand Group basin associated with folding, faulting, and uplift on the margins, particularly in the west, northwest, and north. This tectonic event is termed the Umzawami Event by Dankert and Hein (2010). Unfortunately, such structures were not observed through the seismically transparent package of the Central Rand Group. The preservation of reverse/thrust offsets synchronous to the deposition of the Central Rand Group may have existed in the study area and exhibited offsets that were too small in scale to be imaged by seismics. A well-developed listric fault system was imaged across the study area. The system is constrained as synchronous to the deposition of the Platberg Group and extension during the Hlukana-Platberg event of Manzi et al. (2013).

The Transvaal Supergroup presents a fold system imaged in the seismic sections and is associated with a late to post-Transvaal Supergroup fold event. Dankert and Hein (2010) proposed the formation of a late to post-Transvaal Supergroup fold-thrust belt termed the Ukubambana Event, which they tentatively dated at ca. 2.2–2.0 Ga. Alexandre et al. (2006) provide further refinements to the timing of the fold-thrust belt. Their geochronological $^{40}Ar/^{39}Ar$ dates for syn-kinematic white micas in phyllites placed a deformation event at 2042.1 ± 2.9 Ma. They ascribed the deformation to the formation of the fold-thrust belt, which they named the Transvaalide fold-thrust belt. A second, less well-defined date was also found, referring to an older event at ca. 2150 Ma. The better constrained fold event at 2042.1 ± 2.9 Ma is proposed as being associated with the late to post-Transvaal Supergroup fold event in this study. It is further proposed that the Ukubambana and Transvaalide fold-thrust belts are the same deformation, and that the second name be used in revision, i.e. the Transvaalide Event.

6. Conclusions

In this study we demonstrate the advantages of integrating high-resolution reflection seismic data, borehole data, and surface mapping into a single 3D spatial environment. The integration highlighted new structural relationships that benefited from the creation of a robust 3D spatial platform. This enabled a deeper understanding of both the tectonic history and 3D strato-structural architecture of the Mesoarchaean-Palaeoproterozoic Witwatersrand Basin.

Borehole and surface mapping data were imported into Leapfrog Geo® and together with imported 2D reflection seismic sections, were used to produce wireframes for 3D geological modelling. Twenty eight post-stack migrated 2D reflection seismic sections were available in the study area. Several velocity values, obtained from previous VSP and borehole geophysical surveys conducted in the Witwatersrand Basin, were used to constrain the seismic interpretations. The seismic sections

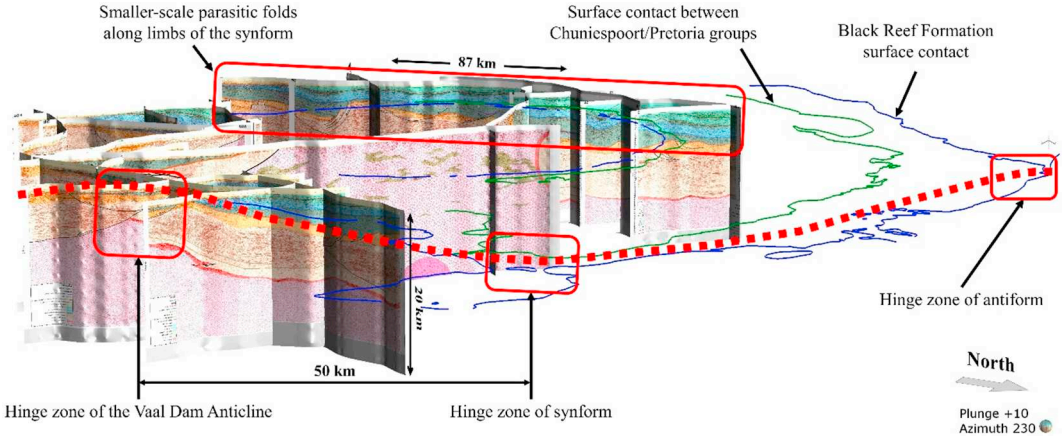

Fig. 14. Estimated geometry of a proposed fold system that combines the imaged folds in the Transvaal Supergroup. The system is illustrated as a main antiform/synform pair, with parasitic folds imaged in the limb of the synform. The proposed antiformal hinge in the north corresponds with mapped outcrop and a change in dip orientation of the Black Reef Formation towards the north. The viewing direction is sub-parallel to the fold axis, i.e. ~230°, providing a cross-sectional view of the synform geometry. The plunge of 10° is not related to the folds but only provides some perspective for the reader.

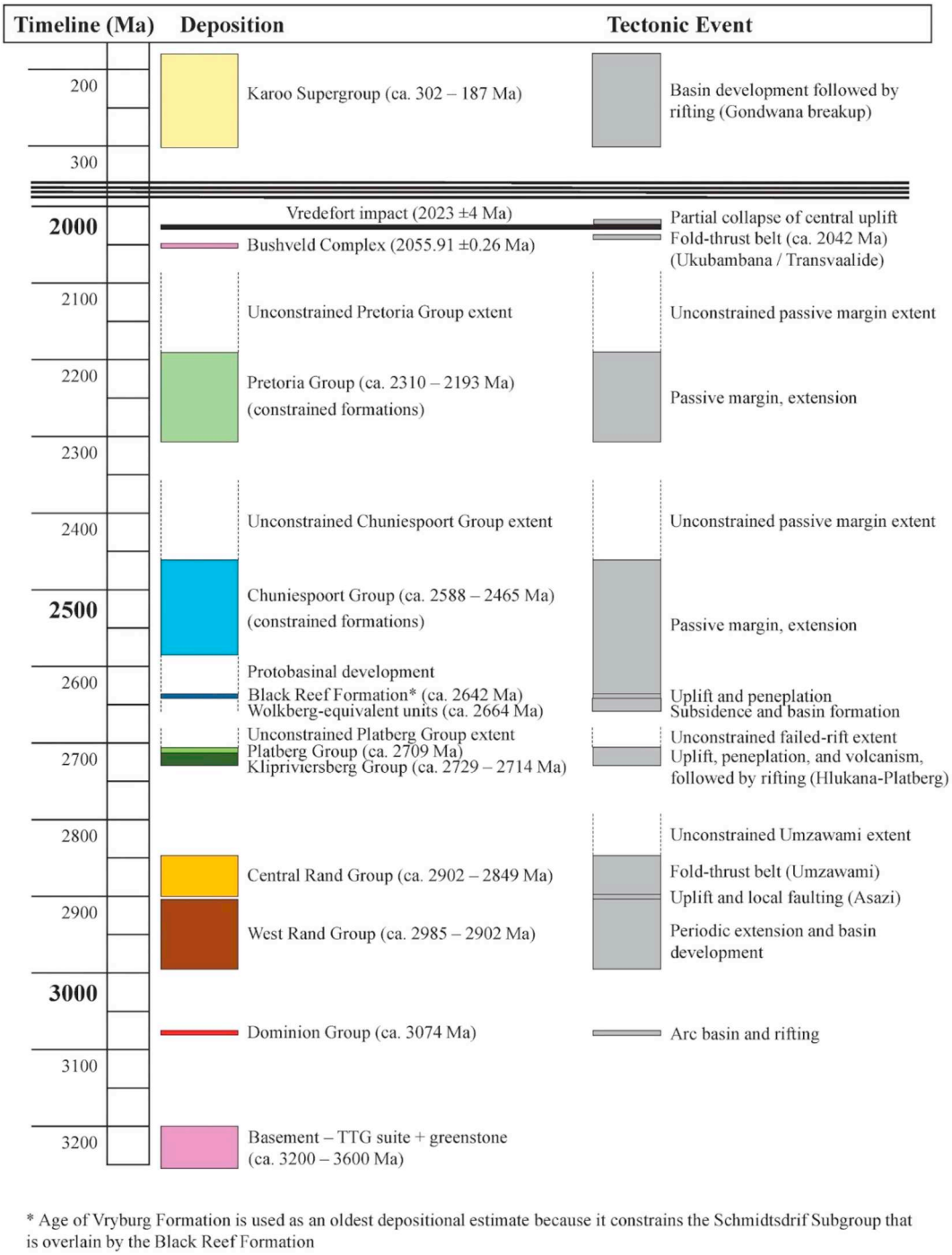

Fig. 15. Schematic chart of deposition and tectonic events for the study area, incorporating findings in this study and published work.

were depth-converted using a constant velocity of 6000 m/s as there was no VSP data or borehole geophysical logs available to constrain more accurate velocity values for depth conversion.

Geological volumes were created for the 3D model using seven major lithological contacts, which were seismically imaged in the study area. The main restrictions on the imaging included the wide coverage of the Karoo Supergroup outcrop, and the relatively sparse, in places shallow, borehole coverage. The elevated basement in the eastern half of the study area is found to form part of a pre-existing basement architecture at the time of the Vredefort impact.

Seven structural features are discussed from the modelling results. These include, (1) a normal fault in the lower West Rand Group, (2) an undulate, normal faulted truncation plane, constrained as post-West Rand Group and pre or early-Central Rand Group, (3) an unconformity and local enhanced uplift constrained as pre to syn-VCF, (4) a listric fault system, constrained as post-Klipriviersberg Group and syn-Platberg Group, (5) an unconformity, constrained as syn-Black Reef Formation, (6) folds, constrained as post-Magaliesberg Formation and pre-Vredefort impact, and (7) a listric fault across the southeastern margin of the Vredefort Dome, constrained as late to post-central uplift formation.

The Asazi Event proposed by Manzi et al. (2013) is supported in the study area. The localised extension observed in some areas provides possible evidence for local scale variation during the deformation process. Due to the seismically transparent Central Rand Group the crosscutting structures in the package were difficult to image, i.e., the

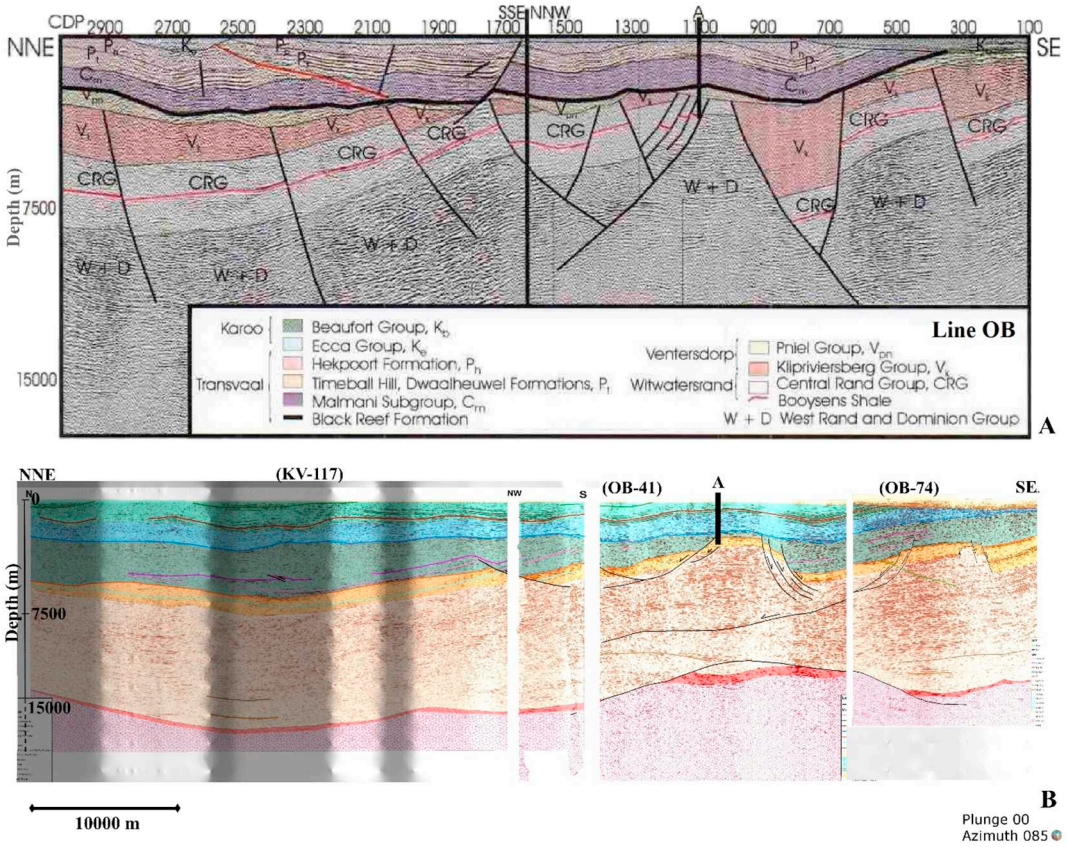

Fig. 16. Interpretation comparison of Line OB from Tinker et al. (2002) with depths referenced to current study. A) Published interpretation (slightly modified) after Tinker et al. (2002) (Fig. 11B in publication). B) Interpretation in this study of the same line (comprising lines KV-117, OB-41, and OB-74) with borehole "A" indicated to guide reference in both images. Note, vertical scale in (B) is in parity with horizontal scale, whereas (A) is vertically exaggerated.

Umzawami Event by Dankert and Hein (2010). The VCF and the Ventersdorp Supergroup exhibit an evolution from enhanced uplift and peneplanation to rift-type extension. Rift-type extension seismically defined in the Ventersdorp Supergroup in several places in the study area supports the Hlukana-Platberg Event of Manzi et al. (2013).

The late to post-Transvaal Supergroup and pre-Vredefort impact fold events proposed by Dankert and Hein (2010) and Alexandre et al. (2006) are supported in this study and assigned to the Transvaalide Event of Alexandre et al. (2006). The large asymmetric, gentle, first-order scale anticline imaged in Domain 2 is associated with this fold

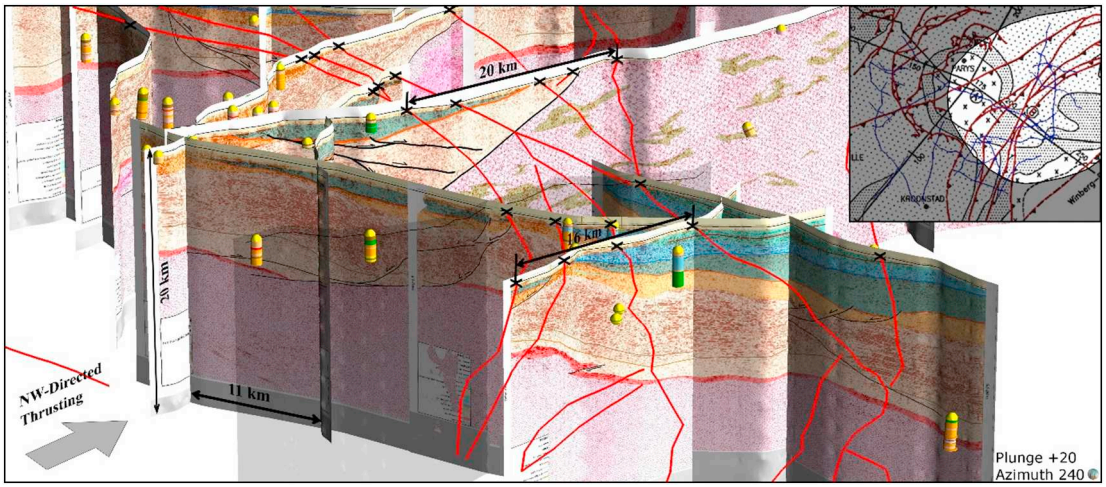

Fig. 17. View of the 2D seismic section interpretations showing an overlay of the northwest-directed thrust fault traces (red) proposed in Figure 27 of Friese et al. (1995). The "X" symbols highlight the surface intersections of the proposed fault traces with the seismic interpretations. Comparisons should only be made where thrust fault traces intersect seismic sections. The inset image shows the area (unshaded) of the original map that is in view here. The blue polylines in the inset indicate the seismic line locations. Boreholes are also included to illustrate the data coverage and are colour-coded by lithology type (note, the yellow markers at the top of each borehole are collar markers). Leapfrog Geo® has no structural symbology for polylines so the northwest thrust direction of these faults is indicated by the grey arrow. For better illustration of these intersections some obstructing seismic sections have been made transparent. (For interpretation of the references to colour in this figure legend, the reader is referred to the web version of this article.)

event and is named here as the Vaal Dam Anticline (VDA).

The seismic section comparisons with Tinker et al. (2002) show comparable structural regimes that depict similar tectonic events. These events include, (1) extensional deformation post-deposition of the Klipriviersberg Group, (2) peneplanation during the Black Reef Formation, and (3) fold development post-deposition of the Hekpoort Formation. One major difference to Tinker et al. (2002) is that the published interpretation does not illustrate the depth association of the faults with an extensional system, as proposed in this study. However due to their significantly limited borehole and high-resolution reflection seismic data, it is suggested that their interpretation was inherently restricted.

The interpretations of thrust faults by Friese et al. (1995) are not supported in this study. Instead the findings in this study suggest that any potential thrust offsets are greatly overshadowed by the larger scale extension-dominated deformation that is absent in their interpretations. The possible thrust-associated uplift in the southeast collar rocks proposed by Friese et al. (1995) is therefore suggested to be of minor importance.

Acknowledgements

The author would like to thank CIMERA (Centre of Excellence for Integrated Mineral and Energy Resource Analysis) for providing both bursary funding and access to software, and the University of the Witwatersrand, Johannesburg, for the Postgraduate Merit Award that covered the registration fees. AngloGold Ashanti is thanked for providing the 2D reflection seismic data. Seismic Micro – Technology (SMT) and Wits Seismic Research Centre for providing licence for the seismic interpretation software. The Council for Geoscience is thanked for providing access to the borehole log archives.

Appendix A. Supplementary data

Supplementary data to this article can be found online at https://doi.org/10.1016/j.tecto.2019.04.004.

References

Alexandre, P., Andreoli, M.A.G., Jamison, A., Gibson, R.L., 2006. 40Ar/39Ar age constraints on low-grade metamorphism and cleavage development in the Transvaal Supergroup (central Kaapvaal craton, South Africa): implications for the tectonic setting of the Bushveld Igneous Complex. S. Afr. J. Geol. 109 (3), 393–410.

Armstrong, R.A., Compston, W., Retief, E.A., Williams, I.S., Welke, H.J., 1991. Zircon ion microprobe studies bearing on the age and evolution of the Witwatersrand triad. Precambrian Res. 53, 243–266.

Beach, A., Smith, R., 2007. Structural geometry and development of the Witwatersrand Basin, South Africa. In: Ries, A.C., Butler, R.W.H., Graham, R.H. (Eds.), Deformation of the Continental Crust: The Legacy of Mike Coward. Special Publications. Geological Society, London, pp. 533–542.

Bumby, A.J., Eriksson, P.G., Catuneanu, O., Nelson, D.R., Rigby, M.J., 2012. Meso-Archaean and Palaeo-Proterozoic sedimentary sequence stratigraphy of the Kaapvaal Craton. Mar. Pet. Geol. 33, 92–116.

Catuneanu, O., Wopfner, H., Erikkson, P.G., Cairncross, B., Rubidge, B.S., Smith, R.M.H., Hancox, P.J., 2005. The Karoo basins of south-central Africa. J. Afr. Earth Sci. 43, 211–253.

Chopra, S., Castagna, J.P., Portniaguine, O., 2006. Seismic resolution and thin-bed reflectivity inversion. CSEG Rec. 31, 19–25.

Coetzee, L.E., 1986. East Rand, Geological Series, Sheet 2628, 1:250,000. Government Printer, Pretoria.

Dankert, B.T., Hein, K.A.A., 2010. Evaluating the structural character and tectonic history of the Witwatersrand Basin. Precambrian Res. 177, 1–22.

De Wet, J.A.J., Hall, D.A., 1994. Interpretation of the Oryx 3D Seismic Survey: Proceedings of the XVth CMMI Congress. vol. 3. South African Institute of Mining and Metallurgy, pp. 259–270.

Farr, T.G., Rosen, P.A., Caro, E., Crippen, R., Duren, R., Hensley, S., Kobrick, S., Paller, M., Rodriguez, E., Roth, L., Seal, D., Shaffer, S., Shimada, J., Umland, J., Werner, M., Oskin, M., Burbank, D., Alsdorf, D., 2007. The Shuttle Radar Topography Mission. Rev. Geophys. 45, RG2004.

Friese, A.E.W., Charlesworth, E.G., McCarthy, T.S., 1995. Tectonic Processes within the Kaapvaal Craton during the Kibaran (Greenville) Orogeny: Constraints from Structural, Geophysical and Isotopic Data in the Witwatersrand Basin and Environs. Information Circular 292. Economic Geology Research Unit, University of the Witwatersrand, Johannesburg, South Africa (67 p).

Frimmel, H.E., 2014. A giant Mesoarchean crustal gold-enrichment episode: possible causes and consequences for exploration. In: Kelley, K., Howard, G. (Eds.), Building Exploration Capability for the 21st Century. Society of Economic Geologists, pp. 209–234 Special Publication No. 18.

Frimmel, H.E., Zeh, A., Lehrmann, B., Hallbauer, D., Frank, W., 2009. Geochemical and geochronological constraints on the nature of the immediate basement next to the Mesoarchaean auriferous Witwatersrand Basin, South Africa. J. Petrol. 50, 2187–2220.

Hanneing, A., Paton, G., 2012. Understanding thin beds using 3D seismic analysis workflows, attributes: new views on seismic imaging – their use in exploration and production. In: 31st Annual GCSSEPM Foundation Bob F. Perkins Research Conference. vol. 1. pp. 322–341.

Henkel, H., Reimold, W.U., 1998. Integrated geophysical modelling of a giant, complex impact structure: anatomy of the Vredefort Structure, South Africa. Tectonophysics 287, 1–20.

Johnson, M.R., Anhaeusser, C.R., Thomas, R.J., 2006. The Geology of South Africa. Jointly by Geological Society of South Africa and Council for Geosciences, Gauteng, South Africa (691 pp).

Jones, M.Q.W., 2003. Thermal properties of stratified rocks from Witwatersrand gold mining areas. J. South. Afr. Inst. Min. Metall. 26 (3), 173–186.

Jones, R.R., McCaffrey, K.J.W., Clegg, P., Wilson, R.W., Holliman, N.S., Holdsworth, R.E., Imber, J., Waggot, S., 2009. Integration of regional to outcrop digital data: 3D visualisation of multi-scale geological models. Comput. Geosci. 35, 4–18.

Kamo, S.L., Reimold, W.U., Krogh, T.E., Colliston, W.P., 1996. A 2.023 Ga age for the Vredefort impact event and a first report of shock metamorphosed zircons in pseudotachylitic breccias and Granophyre. Earth Planet. Sci. Lett. 144, 369–387.

Kaufmann, O., Martin, T., 2009. Reprint of "3D geological modelling from boreholes, cross-sections and geological maps, application over former natural gas storages in coal mines" [Comput. Geosci. 34 (2008) 278–290]. Comput. Geosci. 35, 70–82.

Kositcin, N., Krape˘z, B., 2004. Relationship between detrital zircon age-spectra and the tectonic evolution of the late Archaean Witwatersrand Basin, South Africa. Precambrian Res. 129, 141–168.

Manzi, M.S.D., Durrheim, R.J., Hein, K.A.A., King, N., 2012a. 3D edge detection seismic attributes used to map potential conduits for water and methane in deep gold mines in the Witwatersrand basin, South Africa. Geophysics 77, 133–147.

Manzi, M.S.D., Gibson, M.A.S., Hein, K.A.A., King, N., Durrheim, R.J., 2012b. Application of 3D seismic techniques to evaluate ore resources in the West Wits Line goldfield and portions of the West Rand goldfield, South Africa. Geophysics 77, 163–171.

Manzi, M.S.D., Hein, K.A.A., King, N., Durrheim, R.J., 2013. Neoarchaean tectonic history of the Witwatersrand Basin and Ventersdorp Supergroup: new constraints from high-resolution 3D seismic reflection data. Tectonophysics 590, 94–105.

Manzi, M.S.D., Hein, K.A.A., Durrheim, R.J., King, N., 2014. The Ventersdorp Contact Reef model in the Kloof Gold Mine as derived from 3D seismics, geological mapping and exploration borehole datasets. Int. J. Rock Mech. Min. Sci. 66, 97–113.

Molezzi, M.G., 2017. Modelling the Witwatersrand Basin: A Window Into Neoarchaean-Palaeoproterozoic Crustal-scale Tectonics. Unpublished Master's thesis. University of the Witwatersrand, Johannesburg (223p).

Niu, F., James, D.E., 2002. Fine structure of the lowermost crust beneath the Kaapvaal craton and its implications for crustal formation and evolution. Earth Planet. Sci. Lett. 200, 121–130.

Nkosi, N.Z., Manzi, M.S.D., Drennan, G.R., Yilmaz, H., 2017. Experimental measurements of seismic velocities on core samples and their dependence on mineralogy and stress; Witwatersrand Basin (South Africa). Stud. Geophys. Geod. 61, 115–144.

Phillips, N.G., Law, J.D.M., 1994. Metamorphism of the Witwatersrand gold fields: a review. Ore Geol. Rev. 9, 1–31.

Poujol, M., Robb, L.J., Anhaeusser, C.R., Gericke, B., 2003. A review of the geochronological constraints on the evolution of the Kaapvaal Craton, South Africa. Precambrian Res. 127, 181–213.

Pretorius, D.A., Brink, W.C.J., Fouche, J., 1986. Geological map of the Witwatersrand Basin. In: Anhaeusser, C.R., Maske, S. (Eds.), Mineral Deposits of Southern Africa, vol. I. Geological Society of South Africa, Johannesburg.

Pretorius, C.C., Jamison, A.A., Irons, C., 1987. Seismic exploration in the Witwatersrand Basin, RSA. Exploration '87. In: Proceedings Geophysical Methods: Advances in the State of the Art. vol. 22. pp. 241–253.

Pretorius, C.C., Steenkamp, W.H., Smith, R.G., 1994. Developments in data acquisition, processing and interpretation over ten years of deep vibroseismic surveying in South Africa. In: Proceedings of the 15th Congress of the Council for Mining and Metallurgical Institutions. 3. South African Institute of Mining and Metallurgy, pp. 249–258.

Pretorius, C.C., Trewick, W.F., Irons, C., 2000. Application of 3D seismics to mine planning at the Vaal Reefs gold mine, number 10 shaft, Republic of South Africa. Geophysics 65, 1862–1870.

Pretorius, C.C., Muller, M.R., Larroque, M., Wilkins, C., 2003. A review of 16 years of hardrock seismic of the Kaapvaal Craton. In: Eaton, D.W., Milkereit, B., Salisbury, M.H. (Eds.), Hardrock Seismic Exploration, Geophysical Developments. vol. 10. Society of Exploration Geophysics, pp. 247–268.

Reimold, W.U., Koeberl, C., 2014. Impact structures in Africa: a review. J. Afr. Earth Sci. 93, 57–175.

Retief, P.F., 2000. Kroonstad. Geological Series, Sheet 2726, 1:250,000. Council for Geoscience, Pretoria.

Salisbury, M.H., Harvey, G.W., Mathews, L., 2003. The acoustic properties of ores and host rocks in hardrock terranes. In: Eaton, D.W., Milkereit, B., Salisbury, M.H. (Eds.), Hardrock Seismic Exploration, Geophysical Developments. vol. 10. Society of Exploration Geophysics, pp. 9–19.

Simpson, C., 1978. The structure of the rim syncline of the Vredefort Dome. Trans. Geol. Soc. S. Afr. 81, 115–121.

Smith, R., 1992. Frankfurt, Geological Series, Sheet 2728, 1:250,000. Government

Printer, Pretoria.
Tinker, J., De Wit, M., Grotzinger, J., 2002. Seismic stratigraphic constrained on Neoarchean – Paleoproterozoic evolution of the western margin of the Kaapvaal craton, South Africa. S. Afr. J. Geol. 105, 107–134.
Van Niekerk, C.B., 1962. The age of the Gemspost dyke from the Ventersdorp gold mine. Trans. Geol. Soc. S. Afr. 65, 105–111.
Weder, E.E.W., 1994. Structure of the Area South of the Central Rand Gold Mines as Derived from a Gravity and Vibroseis Surveys: Proceedings of the XVth CMMI Congress. vol. 3. South African Institute of Mining and Metallurgy, pp. 271–281.
Widess, M.B., 1973. How thin is thin bed? Geophysics 38, 1176–1180.
Wilkinson, K.J., 1986. Wes-Rand, Geological Series, Sheet 2626, 1:250,000. Government Printer, Pretoria.